scientific reports

Check for updates

OPEN

Inhibition of free radicals and inflammation on RAW264.7 macrophage cell line by *Arthrospira platensis* extract

Pitchayuth Srisai[1,2], Sureeporn Suriyaprom[2,3], Supakit Khacha-Ananda[4], Aussara Panya[2,7,8], Hans Bäumler[5,6] & Yingmanee Tragoolpua[2,7,8]✉

Inflammation and oxidative stress are key drivers of various diseases. *Arthrospira platensis* is a filamentous cyanobacterium and exhibits significant high nutritional value. Biological activities of *A. platensis* extract (APE) against free radicals and inflammation on LPS-stimulated RAW264.7 cells were investigated in this study. The results showed that APE exhibited high levels of total protein, phycobiliprotein and phenolic compound. LC–MS profiling further confirmed the presence of multiple antioxidant metabolites, including glutathione and ergothioneine. APE exhibited low toxicity toward RAW264.7 cells. The anti-inflammatory activity of APE was evaluated on LPS-stimulated RAW264.7 cells, where it significantly suppressed the expression of the *iNOS* gene and iNOS protein, as well as inhibited NO secretion. Additionally, the anti-inflammatory effects of APE were assessed by measuring the secretion of pro-inflammatory cytokines (TNF-α, IL-6) and the anti-inflammatory cytokine (IL-10) in LPS-stimulated RAW264.7 cells. The results indicated that APE significantly reduced TNF-α and IL-6 levels while increasing IL-10 production, suggesting strong anti-inflammatory potential. Moreover, the ability of APE to inhibit intracellular reactive oxygen and nitrogen species was also investigated. The findings revealed that APE effectively suppressed both reactive oxygen species and reactive nitrogen species on LPS-stimulated RAW264.7 cells. Furthermore, APE significantly reduced lipid peroxidation as indicated by decreased malondialdehyde levels and improved the glutathione redox status. The effects were more pronounced than treatment with exogenous L-glutathione alone, suggesting the synergistic antioxidant capacity of APE. Therefore, these findings highlight the potential of *A. platensis* extract as a functional ingredient for the prevention or management of inflammation and oxidative stress-related conditions.

Inflammation is a fundamental biological response of the immune system to various abnormal conditions, including infections, cellular injuries, or toxic compounds. This response plays a crucial role in host defence by recruiting immune cells to affected tissues and promoting tissue repair. This process is tightly regulated and consists of two primary phases, acute and chronic inflammation[1,2]. Acute inflammation is a rapid and transient response characterized by redness, swelling, heat, and pain, resulting from increased vascular permeability and immune cell infiltration[3]. This response is predominantly mediated by pro-inflammatory cytokines such as tumour necrosis factor-alpha (TNF-α), interleukins (IL) including IL-6 and IL-1β, as well as signalling molecules, e.g., nitric oxide (NO) and reactive oxygen species (ROS). Once the underlying stimulus is neutralized, anti-inflammatory cytokines such as IL-10 and transforming growth factor-beta (TGF-β) restore tissue homeostasis and prevent excessive immune activation[4,5]. On the other hand, chronic inflammation persists over a prolonged

[1]Interdisciplinary Program in Biotechnology, Multidisciplinary and Interdisciplinary School, Chiang Mai University, Chiang Mai 50200, Thailand. [2]Department of Biology, Faculty of Science, Chiang Mai University, Chiang Mai 50200, Thailand. [3]Office of Research Administration, Chiang Mai University, Chiang Mai 50200, Thailand. [4]Department of Forensic Medicine, Faculty of Medicine, Chiang Mai University, Chiang Mai 50200, Thailand. [5]Institute of Transfusion Medicine, Charité-Universitätsmedizin Berlin, 10117 Berlin, Germany. [6]Faculty of Pharmacy, Payap University, Chiang Mai 50210, Thailand. [7]Natural Extracts and Innovative Products for Alternative Healthcare Research Group, Faculty of Science, Chiang Mai University, Chiang Mai 50200, Thailand. [8]Cell Engineering for Cancer Therapy Research Group, Faculty of Science, Chiang Mai University, Chiang Mai 50200, Thailand. ✉email: yingmanee.t@cmu.ac.th; yboony150@gmail.com

period and is associated with various diseases, including autoimmune disorders, cardiovascular diseases, and cancer[6]. Persistent inflammatory signals can lead to tissue damage, fibrosis, and dysregulated immune responses. Several factors, such as infections, environmental stressors, and lifestyle choices, contribute to the transition from acute to chronic inflammation[7,8].

Oxidative and nitrosative stress are critical factors contributing to cellular dysfunction and inflammatory diseases. Excessive production of reactive oxygen species (ROS) and reactive nitrogen species (RNS) can lead to oxidative damage, disrupting cellular homeostasis and promoting the progression of various pathological conditions, including autoimmune disorders, cardiovascular diseases, and cancer[9,10]. Under normal physiological conditions, ROS and RNS play essential roles in cell signalling, immune defence, and homeostasis. However, an imbalance between their production and the antioxidant defence system leads to oxidative stress, triggering inflammatory responses, mitochondrial dysfunction, and cell apoptosis. The overproduction of ROS, such as superoxide anion (O_2^-), hydrogen peroxide (H_2O_2), and hydroxyl radicals ($OH^•$), results in lipid peroxidation, protein oxidation, and DNA damage. Similarly, RNS, including nitric oxide (NO) and peroxynitrite ($ONOO^-$), contribute to nitrosative stress, exacerbating inflammatory signalling and impairing cellular function[11–13].

The treatment of inflammation typically involves the use of modern medications, such as steroidal anti-inflammatory drugs (SAIDs), which belong to the steroid compound group. However, prolonged use of SAIDs can lead to various adverse effects. Alternatively, non-steroidal anti-inflammatory drugs (NSAIDs) are commonly used. While NSAIDs do not contain steroid compounds, they can cause gastrointestinal irritation[14,15]. Natural compounds with anti-inflammatory properties, such as plant extracts, have shown strong potential in modulating immune responses and reducing inflammation[16]. Bioactive compounds derived from cyanobacteria have demonstrated significant anti-inflammatory efficacy by regulating cytokine secretion and inflammatory pathways while exhibiting minimal toxicity to cells and the human body. Unlike synthetic drugs, they do not negatively affect internal organs and offer high safety, making them promising candidates for development into functional food products. Additionally, cyanobacteria are easy to culture, exhibit rapid growth, and contain diverse bioactive proteins with applications in healthcare, agriculture, and medicine[17–19].

Research on cyanobacteria and algae-derived bioactive compounds has revealed various substances with potent biological activities. For instance, eleganonal from *Bifurcaria bifurcate*, fucoxanthin from *Cladosiphon okamuranus*, and diterpene from *Padina tetrastromatic* exhibit antioxidant properties, as demonstrated by the DPPH assay[20–22]. Compounds such as sterol from *Codium fragile*, β-cryptoxanthin from *Dunaliella salina*, and β-carotene and phycocyanin from *Spirulina platensis* display anti-inflammatory activity by suppressing pro-inflammatory cytokine and cytokine genes, including *COX-2*, *iNOS*, *TNF-α*, *IL-1β*, and *IL-6*, while inhibiting pro-inflammatory mediators such as nitric oxide and prostaglandin E2[23,24]. Additionally, *Arthrospira platensis* has been shown to modulate immune responses by enhancing B-cell and T-cell activity, promoting antibody production, and regulating the secretion of specific cytokines[25,26].

Arthrospira (*Spirulina*) *platensis* is one of the most widely cultivated cyanobacteria, recognized as a valuable resource for enhancing food nutrition, improving agricultural applications, and serving as a source of bioactive compounds for nutraceuticals. It is commonly consumed as a health supplement due to its high nutritional value, containing protein, carbohydrates, lipids, and fibre[27]. Additionally, *A. platensis* is a rich source of essential vitamins, including B1, B2, B3, B6, B12, C, and D, as well as β-carotene, a precursor for vitamin A synthesis[28]. It also contains essential minerals and bioactive pigments with potent antioxidant properties, such as carotenes, chlorophyll A, and phycocyanin. Beyond its nutritional applications, *A. platensis* has been utilized in various industries, including livestock farming, cosmetics, pharmaceuticals, and as a fluorescent dye alternative in scientific research[29,30].

Therefore, this study aimed to investigate the anti-inflammatory potential of aqueous extracts of *A. platensis*, with a particular focus on their ability to modulate cytokine production on LPS-stimulated RAW264.7 cells. Additionally, the anti-free radical properties, specifically its capacity to neutralize reactive oxygen species (ROS) and reactive nitrogen species (RNS) were examined.

Materials and methods

A. platensis extracts (APE) preparation

Heat-dried *Arthrospira platensis* powder was kindly provided by Boonsom Farm (Greendiamond Co., Ltd.), Thung Pi Sub-District, Mae Wang District, Chiang Mai, Thailand. *A. platensis* was performed using the maceration technique. Briefly, *A. platensis* powder was immersed in distilled water at a 1:10 (w/v) ratio and incubated at 45 °C for 3 h. The extract was then separated by centrifugation at 4,000 × g for 15 min to obtain supernatant, while the *A. platensis* cells were precipitated. The supernatant was subsequently filtered through Whatman Grade 1 filter paper (pore size 11 µm, diameter 125 mm). The extract solution was concentrated under reduced pressure using a rotary evaporator (Hei-VAP, Heidolph, Germany) and further freeze-dried using lyophilizer (FreeZone, Labconco, USA) to remove the remaining solvent. The lyophilized *A. platensis* extract (APE) was then dissolved in distilled water at a concentration of 200 mg/mL and filtrated through nylon syringe filter pore size 0.45 µm, diameter 13 mm (Labfil, China) prior to use for study of anti-free radicals and anti-inflammatory experiments [31]. A 20 mM solution of L-glutathione in its reduced form (GSH; Sigma-Aldrich, USA) was used as a representative pure compound for comparison, based on its identification in APE through phytochemical profiling. Additionally, 10 µM dexamethasone (DEX; Decton, Thailand) was included as a reference anti-inflammatory control.

Phytochemical profile analysis

The content of polysaccharide, protein, phycobiliproteins, total phenolic compounds, and glutathione in APE was determined using specific colorimetry assay. The polysaccharide was examined as a total carbohydrate content using phenol-sulfuric assay with D-glucose as a standard. 0.5 mL of APE was mixed with 0.5 mL of

5% (w/v) phenol solution. Subsequently, 2.5 mL of 98% (w/w) sulfuric acid was rapidly added directly to the liquid surface. The mixture was vortexed and allowed to stand at room temperature for 10 min. Absorbance of the reaction chromophore was measured at 490 nm using a spectrophotometer (Genesys 20, Thermo Scientific, USA) and the total carbohydrate content was reported as milligrams of D-glucose equivalent per gram of APE (mg D-glucose/g APE)[32].

The protein content was determined by Bradford protein assay using Bio-Rad protein assay dye (Bio-Rad, USA) with bovine serum albumin (BSA) as a standard. Briefly, 10 µL of APE was complexed with 200 µL of protein assay dye reagent. After complexing, the reaction was incubated in darkness for 10 min. Absorbance of the reaction was detected at 595 nm by a microplate reader (Spectra MR, DYNEX Technologies, USA) and the total protein content was expressed as milligrams of BSA equivalent per gram of APE (mg BSA/g APE)[33]. The phycobiliprotein content, including allophycocyanin, phycocyanin, and phycoerythrin was also determined. The absorbance at 562, 615, and 652 nm was measured by a spectrophotometry and the content was calculated using the Bennett and Bogorad equation[34].

The total phenolic content was examined by Folin-Ciocalteu assay with slight modifications. In the assay procedure, 25 µL of APE was combined with 150 µL of Folin-Ciocalteu's reagent and incubated in the dark for 5 min. Subsequently, 100 µL of 7.5% (w/v) sodium carbonate was added, and the mixture was further incubated in the dark for 30 min. The measurement of absorbance was performed at 765 nm using a microplate reader. Gallic acid was used as a reference standard, and the results were expressed as milligrams of gallic acid equivalents per gram of APE (mg GAE/g APE)[35].

Moreover, the L-glutathione content was determined by Ellman's assay using L-glutathione reduced form (GSH) as a standard, with slight modifications. To remove other thiol-containing proteins, 10% trichloroacetic acid was added to precipitate proteins, and the sample was subsequently neutralized with 1 mM NaOH. Then, APE (100 µL) was mixed with 0.1 M phosphate buffer pH 7.0 (100 µL). Then, 50 µL of Ellman's reagent [1 mM 5,5'-dithiobis-(2-nitrobenzoic acid) (DTNB) in phosphate buffer] was added and incubated for 10 min in the dark. The reaction absorbance was measured at 412 nm using a microplate reader[36].

The phytochemical profile of APE was analysed by liquid chromatography-mass spectrometry (LC–MS) with a quadrupole time-of-flight (Q-TOF) mass spectrometer (LC/MS 6545XT AdvanceBio LC/Q-TOF, Agilent Technologies, USA). Chromatographic separation was achieved using an EC-C18 column (2.1 × 100 mm, 2.7 µm, 120 Å; InfinityLab Poroshell 120, Agilent Technologies, USA) and maintained at 50 °C. The mobile phase consisted of 0.1% (v/v) aqueous formic acid (solvent A) and 0.1% (v/v) formic acid in acetonitrile (solvent B). The elution was carried out at a flow rate of 0.4 mL/min with a gradient elution program over 20 min. The injection volume was 10 µL. Mass spectrometry was performed in both positive and negative electrospray ionization (ESI) modes under high-resolution settings. The mass spectrometer was operated with a drying gas temperature of 325 °C with a flow rate of 13 L/min, sheath gas temperature of 275 °C with a flow rate of 12 L/min, nebulizer pressure at 45 psi, and capillary voltage set at + 4000 V/−3000 V. Data were acquired within an m/z range of 40–1700 for MS1 and 25–1000 for MS2 using a collision energy of 20 eV in positive mode and 10 eV in negative mode. The acquired data were processed using MS-DIAL version 5.3 (RIKEN CSRS, Japan), and data normalization was conducted using sulfadimethoxine as an internal standard. Metabolite identification was carried out using MS-DIAL's in-house ESI (+/−) MS/MS library from authentic standards[37,38].

Cell culture and leukocytes isolation

The murine macrophage cell line RAW264.7 (ATCC-TIB-71) originating from *Mus musculus*, was purchased from the American Type Culture Collection (ATCC). The cells were cultured as a monolayer in Dulbecco's modified Eagle medium (DMEM; Gibco, UK) supplemented with 10% (v/v) heat-inactivated fetal bovine serum (FBS; Gibco, UK), 100 µg/mL streptomycin and 100 U/mL penicillin (Gibco, UK), and 10 mM of 4-(2-hydroxyethyl)-1-piperazineethanesulfonic acid (HEPES). The cells were maintained at 37 °C in a humidified 5% (v/v) CO_2 incubator until they reached 80–90% confluence (approximately 2–3 days).

Human leukocytes, including peripheral blood mononuclear cells (PBMCs) and polymorphonuclear leukocytes (PMNs), were isolated from the blood of healthy donors using Histopaque (Sigma-Aldrich, USA). Venous blood was collected from volunteer donors and anticoagulated with lithium heparin. The operate of donor blood samples for scientific purposed was approved by the ethics committee of the Charité-Universitätsmedizin Berlin (EA1/110/21). All experimental procedures involving human participants were performed in accordance with relevant guidelines and regulations, and informed consent was obtained from all subjects. The blood was diluted 1:1 with Dulbecco's phosphate-buffered saline (DPBS) and gently layered over a double gradient of Histopaque-1077 and Histopaque-1119 (with Histopaque-1077 layer over the Histopaque-1119 layer) in equal volumes. The gradient was centrifuged at 700 × g for 30 min, and the buffy coat was carefully harvested. PBMCs were collected from the interface between the plasma and Histopaque-1077, while PMNs were obtained from the interface between the Histopaque-1077 and Histopaque-1119. The cells were washed twice with 10 mL DPBS and centrifuged at 300 × g for 10 min to remove residual DPBS. The cell pellets were then resuspended in Roswell Park Memorial Institute 1640 medium (RPMI-1640; Gibco, UK) supplemented with 10% (v/v) of heat-inactivated FBS, 0.2 mM glutamine, and 100 µg/mL streptomycin and 100 U/mL penicillin. The freshly isolated human leukocytes were used immediately after isolation.

Cell viability assay

The cytotoxic effect of *A. platensis* extract (APE) on RAW264.7 cells was assessed using the 3-(4,5-dimethylthiazol-2-yl)-2,5-diphenyl-tetrazolium bromide (MTT) assay. RAW264.7 cells were grown at a density of 1×10^5 cells/well in a 96-well plate for 24 h. APE was prepared in DMEM growth medium, and the cells were treated with various concentrations of APE (0, 125, 250, 500, 1000, and 2000 µg/mL) before incubation at 37 °C in a CO_2 incubator for 24 h. After incubation, the MTT assay (Bio Basic, Canada) was performed according to

the manufacturer's instructions. The resulting MTT-formazan product was dissolved in dimethyl sulfoxide (DMSO), and its absorbance was measured at 540 nm with a reference wavelength of 630 nm using a microplate reader. The percentage of cell viability was calculated as the ratio of the absorbance value of treated cells to that of untreated cells.

The cytotoxic effect of APE on normal human cells were evaluated *ex vivo* using the alamarBlue assay. Peripheral blood mononuclear cells (PBMCs) and polymorphonuclear leukocytes (PMNs) were seeded at a density of 1×10^5 cells/well in a black 96-well plate and incubated for 24 h. The cells were then treated with APE at the same concentration range (0, 125, 250, 500, 1000, and 2000 µg/mL) and incubated at 37 °C in a CO_2 incubator for 24 h. Following incubation, the alamarBlue assay (Thermo Scientific, USA) was performed according to the manufacturer's instructions. The red fluorescent resorufin product generated by viable cells was detected using a fluorescence microplate reader (Cytation 3, BioTek Instruments, Germany) with excitation at 560 nm and emission at 590 nm. The percentage of cell viability was calculated as the ratio of the fluorescent intensity of treated cells to that of untreated cells[39,40].

Total RNA extraction and quantitative reverse transcription polymerase Chain reaction (qRT-PCR)

The effect of APE on pro-inflammatory cytokine gene expression from LPS-stimulated RAW264.7 cells was determined using a qRT-PCR assay. RAW264.7 cells were cultured at a density of 5×10^5 cells/well in a 12-well plate for 24 h. After that, the medium was replaced with fresh medium containing 1 µg/mL *Escherichia coli* O111:B4 lipopolysaccharides (LPS; Sigma-Aldrich, USA). The stimulated cells were then treated with non-toxic concentrations of APE. L-glutathione reduced form (GSH) was applied as an antioxidant compound and dexamethasone (DEX) was used as a reference control anti-inflammatory agent. The treated cells were incubated at 37 °C in a CO_2 incubator for 24 h.

Total RNA was extracted from the cells using TRIzol reagent (Invitrogen, USA), following the manufacturer's instructions. The isolated RNA was quantified using a microvolume UV–Vis spectrophotometer (NanoDrop One^C, Thermo Scientific, USA). Subsequently, 1 µg of total RNA was converted into complementary DNA (cDNA) by reverse transcription using ReverTra Ace (Toyobo, Japan) in a thermal cycler (Biometra, Analytik Jena, Germany). Afterward, the expression of *TNF-α*, *iNOS*, and *IL-6* genes was analysed from cDNA using the qPCR amplification method by THUNDERBIRD SYBR qPCR Master Mix (Toyobo, Japan). The primers (Bio Basic Asia Pacific, Singapore) for all genes were used as shown in Table 1. The qPCR reaction system contained 10% (v/v) cDNA solution, 0.4 µM sense primer, 0.4 µM antisense primer, and THUNDERBIRD SYBR qPCR Master Mix. The reaction was performed under the following three-step cycling conditions : an initial denaturation at 95.0 °C for 1 min, followed by 40 cycles of denaturation at 95 °C for 15 s, annealing at 60 °C for 15 s, and extension at 72 °C for 30 s, using a quantitative thermal cycler system (qTOWER3 G, Analytik Jena, Germany). The amplification results were expressed as the threshold cycle (Ct) value, which represents the number of cycles required to generate a fluorescent signal exceeding a predefined threshold. The expression levels of *TNF-α*, *iNOS*, and *IL-6* genes were normalized using the *β-actin* gene as an internal control. Relative gene expression was calculated using the comparative Ct method ($2^{-\Delta\Delta Ct}$)[41].

Western blotting analysis

The effect of APE on inducible nitric oxide synthase (iNOS) protein expression in LPS-stimulated RAW264.7 cells was determined by western blotting assay. RAW264.7 cells were cultured at a density of 5×10^5 cells/well in a 12-well plate for 24 h. After incubation, the cells were stimulated using 1 µg/mL LPS, and the stimulated cells were then treated with non-toxic concentrations of APE, GSH and DEX as a reference control. The treated cells were incubated at 37 °C in a CO_2 incubator for 24 h.

The treated cells were lysed with radioimmunoprecipitation assay (RIPA) buffer [50 mM Tris–HCl (pH 8.0), 0.05 mM EDTA, 1% (v/v) Triton X-100, 0.1% (w/v) SDS, and 150 mM NaCl] containing protease inhibitor cocktails (Merck, USA) with a ratio of 1:1000. Cell lysates were centrifuged at 13,000 × g for 20 min. Supernatants were collected, and protein concentration was determined using BCA protein assay reagent (Merck, USA). Proteins from each treatment conditions were resolved by 15% (w/v) sodium dodecyl sulfate–polyacrylamide gel electrophoresis (SDS-PAGE) using a vertical electrophoresis system (Mini-PROTEAN, Bio-Rad, USA). SDS-PAGE was performed at 60 volt (V) for 3 h 30 min to separate proteins, followed by transferred to polyvinylidene fluoride (PVDF) membranes (Merck, USA) using a semi-dry transfer system (Trans-Blot SD, Bio-Rad, USA) at

Gene	Primer	Sequences (5'→3')	Gene bank accession number
TNF-α	Sense	AGCCCCCAGTCTGTATCCTTC	BC117057.1
	Antisense	CATTCGAGGCTCCAGTGAATTCG	
IL-6	Sense	GCTGGAGTCACAGAAGGAGTG	BC132458.1
	Antisense	GCATAACGCACTAGGTTTGCC	
iNOS	Sense	TTCCAGAATCCCTGGACAAGC	U43428.1
	Antisense	TGGTCAAACTCTTGGGGTTCG	
β-actin	Sense	TGCTGTCCCTGTATGCCTCTG	NM_007393
	Antisense	GCTGTAGCCACGCTCGGTCA	

Table 1. The primers used for quantitative PCR analysis.

20 V and 200 milliampere (mA) for 45 min. The membrane was incubated with 5% (w/v) non-fat dried milk as a blocking solution and then probed with the indicated primary antibodies (Merck, USA), including anti-iNOS (1:2000) and anti-β-actin (1:2000). The membranes were then incubated with horseradish peroxidase-conjugated secondary antibody (1:3000). Detection of antibody-specific proteins was performed using an enhanced chemiluminescence reagent (Merck, USA). The chemiluminescent signal was detected by 10–120 s exposure using a chemiluminescent imaging system (ImageQuant LAS 500, GE HealthCare, USA). The expression levels of pro-inflammatory cytokine protein were calculated from densities of iNOS protein, using β-actin protein as a normalizing control (NC)[41].

Measurement of pro-inflammatory and anti-inflammatory cytokine secretion

The effect of APE on pro-inflammatory cytokine and anti-inflammatory cytokine secretion from LPS-stimulated RAW264.7 cells was measured using an enzyme-linked immunosorbent assay (ELISA) kit. TNF-α and IL-6 were analysed as key pro-inflammatory cytokine, while IL-10, a cytokine synthesis inhibitory factor (CSIF), was studied as the main anti-inflammatory cytokine. RAW264.7 cells were plated at a density of 1×10^5 cells/well in a 96-well plate for 24 h. The cells were stimulated using 1 μg/mL LPS, followed by treatment with non-toxic concentrations of APE, GSH and DEX as a reference control. The treated cells were incubated at 37 °C in a CO_2 incubator for 24 h. Cytokine levels (TNF-α, IL-6, and IL-10) were measured from cell culture supernatant using ELISA kits according to the manufacturer's instructions (KOMA Biotech, Korea). Absorbance was measured at 450 nm using an ELISA microplate spectrophotometer (Spectra MR, DYNEX Technologies, USA). The levels of cytokines secreted by RAW264.7 cells were interpolated based on the standard curve provided in the ELISA kit.

Determination of nitric oxide production

The inhibitory effects of APE on nitric oxide (NO) production in LPS-stimulated RAW264.7 cells were determined using nitrite assay. RAW264.7 cells were cultured at a density of 1×10^5 cells/well in a 96-well plate and incubated for 24 h. The cells were then stimulated with 1 μg/mL LPS, followed by treatment with non-toxic concentrations of APE, GSH and DEX as a reference control. The treated cells were incubated at 37 °C in a CO_2 incubator for 24 h. After incubation, the nitric oxide levels in the cell culture supernatant were measured using the Griess reagent. The supernatant was mixed with an equal volume of Griess reagent [1% (w/v) sulfanilamide, 5% (v/v) phosphoric acid, and 0.1% (w/v) N-(1-Naphthyl) ethylenediamine dihydrochloride] and incubated for 10 min. Absorbance was measured at 550 nm using a microplate spectrophotometer. The amount of nitrite in the samples was interpolated based on a sodium nitrite standard curve[42].

Analysis of intracellular reactive oxygen and nitrogen species (RONS) formation

The inhibitory effects of APE on intracellular reactive oxygen and nitrogen species (RONS) level from LPS-stimulated RAW264.7 cells were quantified using a spectrofluorimetric assay and flow cytometry assay. The assays utilized a ROS-sensitive fluorescence indicator, 2',7'-dichlorodihydrofluorescein diacetate (DCFH-DA; Sigma-Aldrich, USA), and an RNS-sensitive fluorescence indicator, 3-amino, 4-aminomethyl-2',7'-difluorofluorescein diacetate (DAF-FM DA; Sigma-Aldrich, USA).

For the spectrofluorimetric assay, RAW264.7 cells were cultured at a density of 1×10^5 cells/well in a 96-well black plate and incubated for 24 h. The cells were then stimulated with 1 μg/mL LPS, followed by treatment with non-toxic concentrations of APE, GSH and DEX as a reference control. The treated cells were incubated at 37 °C in a CO_2 incubator for 24 h. After incubation, the cells were washed twice with Dulbecco's phosphate-buffered saline (DPBS) and loaded with either 20 μM DCFH-DA solution or 10 μM DAF-FM DA reagent. The RONS detection reactions were incubated at 37 °C in the dark for 30 min. The cells were then washed twice, and the solution was replaced with DPBS. Fluorescence signals were measured at 500 nm excitation and 525 nm emission for intracellular ROS levels, and at 495 nm excitation and 515 nm emission for intracellular RNS levels, using multi-mode microplate reader (SpectraMax iD3, Molecular Devices, USA).

For the flow cytometry assay, the cells were cultured at a density of 5×10^5 cells/well in a 12-well plate and incubated for 24 h. The cells were then stimulated with 1 μg/mL LPS, followed by treatment with non-toxic concentrations of APE. The treated cells were incubated at 37 °C in a CO_2 incubator for 24 h. After incubation, the cells were harvested and centrifuged at $300 \times g$ for 10 min. The pellet was washed twice and resuspended in DPBS. The cell suspensions were then incubated with 20 μM DCFH-DA solution or 10 μM DAF-FM DA reagent and incubated at 37 °C in darkness for 30 min. After incubation, the cells were washed twice with DPBS, and the fluorescence signals were analysed using flow cytometry with an excitation wavelength of 488 nm and the emission wavelength of 525 nm on a CytoFLEX flow cytometer (Beckman Coulter, USA). Flow cytometry data were analysed by CytExpert software (Beckman Coulter, USA). The percentage inhibition of RONS was calculated based on the ratio of fluorescent intensity and the number of detected cells between treated and untreated samples[43,44].

Examination of oxidative stress

The effect of APE on oxidative stress in LPS-stimulated RAW264.7 cells were assessed by measuring malondialdehyde (MDA) levels via the thiobarbituric acid reactive substances (TBARS) assay, and by evaluation of intracellular glutathione status (GSH and GSSG levels). RAW264.7 cells were cultured at a density of 5×10^5 cells/well in a 12-well plate for 24 h. After incubation, the cells were stimulated using 1 μg/mL LPS, and the stimulated cells were treated with non-toxic concentrations of APE, GSH and DEX as a reference control. The treated cells were incubated at 37 °C in a CO_2 incubator for 24 h. After incubation, the treated cells were lysed with 0.1 M phosphate buffer pH 7.4 containing protease inhibitor cocktails (Merck, USA), followed sonication technique on ice for 1 min using ultrasonic homogenizer sonicator (CPX600, Ultrasonic Processor, Cole-

Parmer, USA). Cell lysates were centrifuged at 13,000 × g for 20 min. Supernatants were collected, and protein concentration was determined using BCA protein assay reagent.

For TBARS assay, 20 µL of the cell lysate was mixed with 20 µL of 8.1% (w/v) sodium dodecyl sulfate, 150 µL mL of 20% (v/v) acetic acid (pH 3.5), and 150 µL of 0.8% (w/v) thiobarbituric acid (TBA) solution. The mixture was incubated at 95 °C in water bath for 60 min to allow the formation of the MDA-TBA adduct. After cooling to room temperature, 100 µL of distilled water and 500 µL of a butanol:pyridine mixture (15:1) were added. The reaction was centrifuged at 4,000 rpm for 10 min. The upper organic phase was collected, and absorbance was measured at 532 nm using a spectrophotometer. The MDA concentration was calculated based on a standard curve prepared from 1,1,3,3-tetramethoxypropane and expressed as nmol of MDA per milligrams of protein[45].

For glutathione (GSH) and glutathione disulfide (GSSG) levels, the total glutathione (GSHt) and GSSG were measurement using L-glutathione reduced from (GSH) as a standard. To measurement GSHt, 50 µL of the cell lysate was mixed with a reaction mixture containing 100 mM potassium phosphate buffer (pH 7.5), 0.5 mM EDTA, 0.6 mM 5,5′-dithiobis-(2-nitrobenzoic acid) (DTNB), 0.2 mM NADPH, and 0.5 U/mL glutathione reductase. The formation of the TNB product was measured with absorbance at 412 nm for 5 min. GSH levels were normalized to protein content and expressed as nmol of GSH pre milligrams of protein. To determine GSSG, free GSH in the sample was derivatized with 2-vinylpyridine at room temperature for 1 h. The derivatized samples were assayed in the same manner as GSHt. The concentration of GSH was calculated by subtracting twice the amount of GSSG from the total glutathione, as follows: GSH = GSHt – 2GSSG[46,47].

Statistical analysis

The bar graphs and statistical analyses were generated using Prism 10 software (GraphPad Software, USA). Statistical significance among groups was determined using one-way analysis of variance (ANOVA) followed by Dunnett's multiple comparisons test. A p-value of less than 0.05 ($p < 0.05$) was considered statistically significant.

Results

Phytochemical profile of APE

The biochemical composition of APE was quantified using specific colorimetric assays, with the results presented in Table 2. The total carbohydrate content was observed to be 172.89 ± 9.52 mg D-glucose/g APE, indicating a slightly polysaccharide and glucose concentration in the extract (approximately 17%). The total protein content was found to be 548.50 ± 4.53 mg BSA/g APE, indicating a high protein concentration in the extract (approximately 55%). The analysis of phycobiliproteins; phycocyanin and allophycocyanin were the most abundant, with concentrations of 71.99 ± 0.33 mg/g APE and 20.24 ± 0.03 mg/g APE, respectively. Phycoerythrin was also detected in lower amounts with concentrations of 7.66 ± 0.04 mg/g APE. These pigments are known to have antioxidant and light-harvesting properties in cyanobacteria. The L-glutathione content in APE was measured at 31.78 ± 2.76 mg/g APE. Additionally, the extract exhibited a high level of total phenolic compounds, with a concentration of 10.65 ± 1.10 mg GAE/g APE, which are associated with antioxidant activity.

Based on chemical profile analysis of APE using LC–MS, the total ion chromatogram revealed a wide range of metabolites that was eluted at various retention times. Ten putative metabolites were identified with high confidence showing high identification scores (≥ 1.70). The list of identified metabolites is shown in Table 3.

The results showed that the highest identification score was observed for adenine (score = 1.79), indicating a highly reliable identification. Other nucleotides and nucleotide derivatives were also detected. Moreover, the APE contained several amino acids and their derivatives, including phenylalanine, valine, leucine, and norvaline. In addition, antioxidant-related compounds such as L-(+)-ergothioneine and glutathione were identified.

Cytotoxic effects of APE on RAW264.7 cells, human PBMCs, and human PMNs

The cytotoxic effects of APE on RAW264.7 macrophage cells and human leukocytes, including peripheral blood mononuclear cells (PBMCs) and polymorphonuclear cells (PMNs), were evaluated following 24 h treatment at various concentrations of APE (250, 500, 1000, 2000, and 4000 µg/mL). The results demonstrated that APE exhibited low cytotoxicity toward RAW264.7 cells, with cell viability consistently remaining above 80% for APE concentrations up to 2000 µg/mL. However, at the highest concentration of 4000 µg/mL, cell viability significantly decreased to approximately 78.86% (Fig. 1A). Moreover, APE exhibited a dose-dependent cytotoxic effect on human leucocytes. Thus, APE showed significant cytotoxicity toward both PBMCs and PMNs compared to the control group, with PBMCs being more sensitive to APE (Fig. 1B). At concentrations greater

Component	Content
Total carbohydrate content	172.89 ± 9.52 mg D-glucose/g APE
Total protein content	548.50 ± 4.53 mg BSA/g APE
Phycobiliprotein content	
- Allophycocyanin	20.24 ± 0.03 mg/g APE
- Phycocyanin	71.99 ± 0.33 mg/g APE
- Phycoerythrin	7.66 ± 0.04 mg/g APE
L-Glutathione	31.78 ± 2.76 mg/g APE
Total phenolic compounds	10.65 ± 1.10 mg GAE/g APE

Table 2. Quantification of protein, phycobiliproteins, L-glutathione, and total phenolic compounds in APE.

Putative metabolite name	RT (min)	m/z	Adduct ion	Score
Adenine	2.308	136.06668	$[M+H]^+$	1.79
Phenylalanine	3.686	166.08580	$[M+H]^+$	1.78
Valine	2.556	118.08582	$[M+H]^+$	1.78
L-(+)-Ergothioneine	0.749	230.09877	$[M+H]^+$	1.76
Guanine	2.349	152.05617	$[M+H]^+$	1.76
Norvaline	3.225	118.06467	$[M+H]^+$	1.75
Leucine	3.424	132.10150	$[M+H]^+$	1.73
Glutathione	1.070	308.09036	$[M+H]^+$	1.73
L-Pyroglutamic acid	3.424	130.04932	$[M+H]^+$	1.72
Hypoxanthine	1.164	137.04874	$[M+H]^+$	1.70

Table 3. Identification of metabolites in APE by LC–MS analysis. The table lists the putative metabolite name, retention time (RT), mass-to-charge ratio (m/z), adduct ion, chemical ontology, and identification score. Candidate metabolites with high confidence scores (≥ 1.70) are presented.

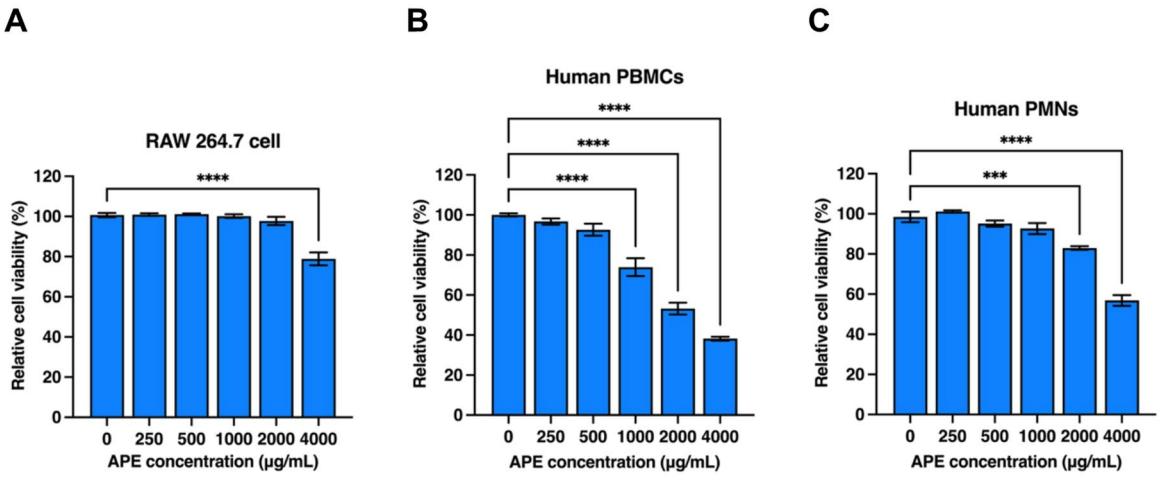

Fig. 1. Effect of APE on cell viability of RAW264.7 cells (**A**), human PBMCs (**B**), and human PMN (**C**). Cells were treated with the indicated concentration of APE (250, 500, 1000, 2000, and 4000 μg/mL) for 24 h. The viability of RAW264.7 cells was assessed using the MTT assay, while the viability of human PBMCs and PMNs was determined using the alamarBlue assay. Results are expressed as the relative percentage of surviving cells compared to control cells. Each value represents the mean ± SEM ($n = 3$). Asterisk indicates significant difference, * ($p \leq 0.05$), ** ($p \leq 0.01$), *** ($p \leq 0.001$) and **** ($p \leq 0.0001$).

than 1000 μg/mL, PBMCs viability decreased by more than 20%. Similarly, PMNs exhibited higher sensitivity to APE (Fig. 1C), with a significant decline in cell viability at concentrations exceeding 2,000 μg/mL. Therefore, APE at concentrations of 500, 1000, and 2000 μg/mL were used to study its effects on inflammation and free radicals in LPS-stimulated RAW264.7 cells. In addition, APE at concentrations of 2000 μg/mL exhibited low toxicity toward normal human blood cells, with a cell viability rate of more than 50%.

Effect of APE on pro-inflammatory cytokine gene expression in LPS-stimulated RAW264.7 cells

The effect of APE on the relative mRNA expression levels of pro-inflammatory cytokine genes, including *TNF-α*, *IL-6*, and *iNOS* genes, in LPS-stimulated RAW264.7 cells was investigated. Cells were pre-treated with lipopolysaccharide (LPS) for 30 min to induce an inflammatory response and then exposed to various concentrations of APE (500, 1000, and 2000 μg/mL) for 24 h. The results were measured using qRT-PCR to quantify the mRNA levels of the targeted genes. The Fig. 2 represents the reduction in the expression levels of the *TNF-α* gene (Fig. 2A), *IL-6* gene (Fig. 2B), and *iNOS* gene (Fig. 2C) in a dose-dependent manner. The highest concentration of APE (2000 μg/mL) exhibited the most substantial inhibitory effect by significantly decreasing the gene expression of all pro-inflammatory cytokine gene compared to the LPS-stimulated cell group and 10 μM dexamethasone (DEX). Similarly, the L-glutathione (GSH) treatment also significantly reduced the expression of TNF-α (Fig. 3A) and iNOS (Fig. 3C) in a dose-dependent manner. However, GSH did not significantly inhibit IL-6 expression (Fig. 3B).

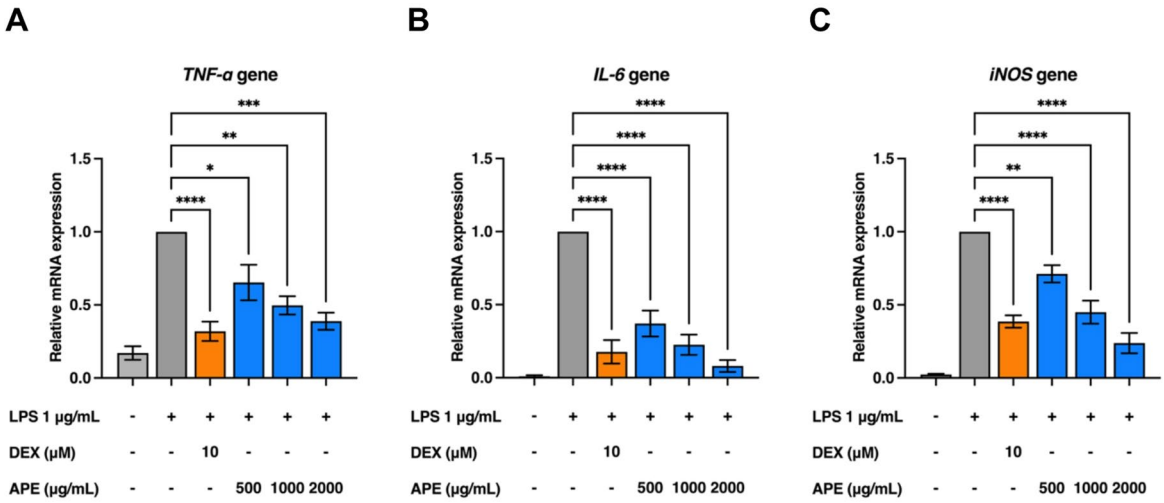

Fig. 2. Effects of APE on the gene expression of pro-inflammatory cytokine such as *TNF-α* (**A**), *IL-6* (**B**), and *iNOS* (**C**) in LPS-stimulated RAW264.7 cells and dexamethasone (DEX) as a reference control. Cells were stimulated with LPS for 30 min and then treated with APE (500–2000 μg/mL) or 10 μM DEX for 24 h. The mRNA expression levels were measured using qRT-PCR. Results are represented as the relative mRNA expression compared to LPS-stimulated cell group. Each value represents the mean ± SEM ($n = 3$). Asterisk indicates significant difference, * ($p \leq 0.05$), ** ($p \leq 0.01$), *** ($p \leq 0.001$) and **** ($p \leq 0.0001$).

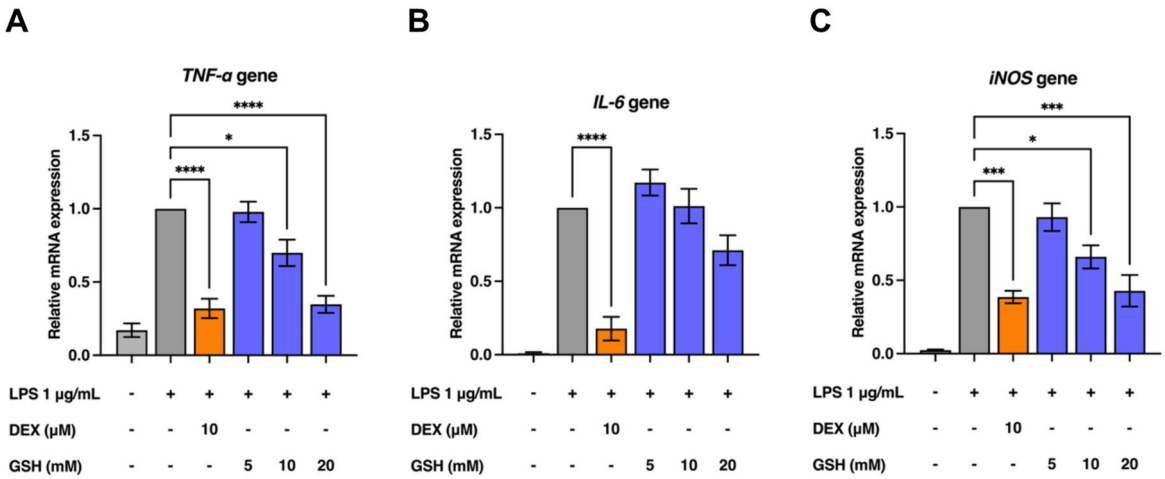

Fig. 3. Effects of GSH on the gene expression of pro-inflammatory cytokine such as *TNF-α* (**A**), *IL-6* (**B**), and *iNOS* (**C**) in LPS-stimulated RAW264.7 cells and dexamethasone (DEX) as a reference control. Cells were stimulated with LPS for 30 min and then treated with GSH (5–20 mM) or 10 μM DEX for 24 h. The mRNA expression levels were quantified by qRT-PCR. Results are represented as the relative mRNA expression compared to LPS-stimulated cell group. Each value represents the mean ± SEM ($n = 3$). Asterisk indicates significant difference, * ($p \leq 0.05$), ** ($p \leq 0.01$), *** ($p \leq 0.001$) and **** ($p \leq 0.0001$).

Effect of APE on iNOS protein expression in LPS-stimulated RAW264.7 cells

The effect of APE on the relative protein expression of iNOS in LPS-stimulated RAW264.7 cells was assessed through both bar chart analysis (Fig. 4A) and western blot assay (Fig. 4B). The corresponding uncropped raw blot images are provided in *Supplementary Data*. Cells were pre-treated with LPS (1 μg/mL) for 30 min to induce an inflammatory state, followed by treatment with varying concentrations of APE (62.5, 125, 250, 500, 1000, and 2000 μg/mL) for 24 h. APE demonstrated a dose-dependent decrease in iNOS protein expression levels with increasing APE concentrations. The highest concentration of APE (2000 μg/mL) resulted in the most significant reduction in iNOS protein expression compared to the LPS-stimulated control.

The corresponding western blot bands were normalized using β-actin as a control. The iNOS protein band intensity in LPS-stimulated cells was notably stronger than that in the non-stimulated control cells, confirming successful induction of iNOS expression by LPS. Treatment with APE showed a gradual attenuation of iNOS protein band intensity as the concentration of APE increased. These results suggest that APE can modulate

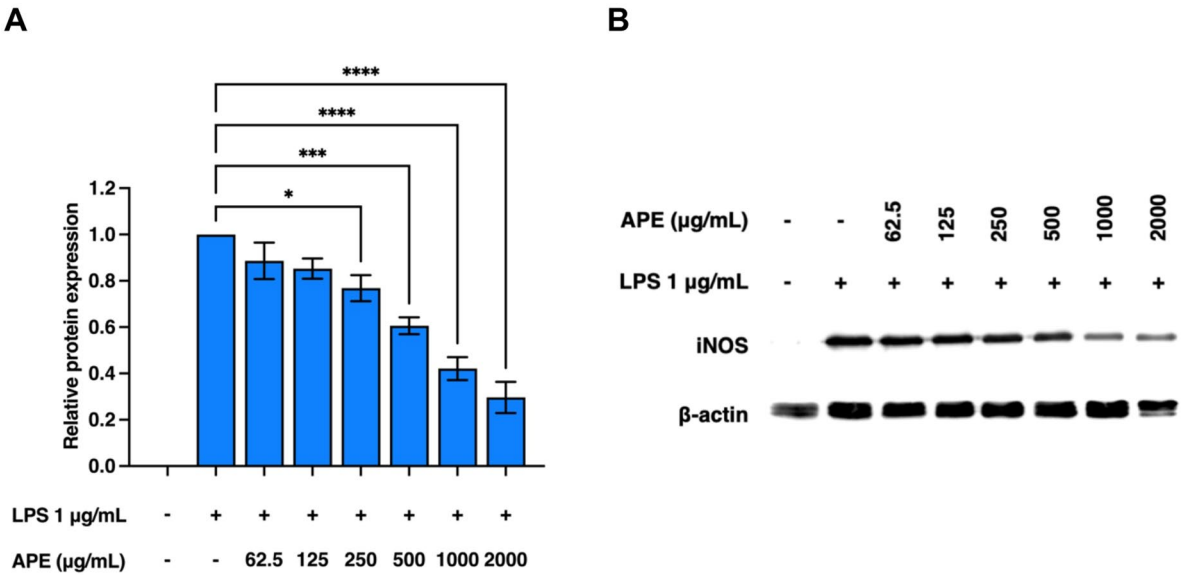

Fig. 4. Effects of APE on iNOS protein expression in LPS-stimulated RAW264.7 cells (**A**). Cells were stimulated with LPS for 30 min and then treated with non-toxic concentrations of APE for 24 h. The iNOS protein expression levels were measured by western blotting (**B**). Results are presented as relative protein expression compared to the LPS-stimulated cell group. Each value represents the mean ± SEM ($n = 3$). Asterisk indicates significant difference, * ($p \leq 0.05$), ** ($p \leq 0.01$), *** ($p \leq 0.001$) and **** ($p \leq 0.0001$).

LPS-stimulated inflammatory responses in RAW264.7 cells by downregulating iNOS protein expression in a concentration-dependent manner. This effect highlights the potential anti-inflammatory properties of APE and its ability to interfere with the signalling pathways involved in the overexpression of iNOS during inflammation in LPS-stimulated cell model.

Effect of APE on pro-inflammatory and anti-inflammatory cytokine secretion in LPS-stimulated RAW264.7 cells

The effects of APE on the secretion levels of pro-inflammatory cytokines TNF-α and IL-6, as well as the anti-inflammatory cytokine IL-10, in LPS-stimulated RAW264.7 macrophage cell were examined. Cells were first stimulated with 1 μg/mL of LPS for 30 min to induce an inflammatory response, followed by treatment with varying concentrations of APE (500, 1000, and 2000 μg/mL) for 24 h. Cytokine levels were measured using an ELISA kit. The results revealed a significant elevation of TNF-α and IL-6 in the LPS-stimulated group compared to the untreated control. Effects of APE on the secretion of pro-inflammatory cytokines, including TNF-α (Fig. 5A) and IL-6 (Fig. 5B), as well as the anti-inflammatory cytokine IL-10 (Fig. 5C) in LPS-stimulated RAW264.7 cells. LPS stimulation significantly increased the secretion of TNF-α and IL-6, indicating a strong inflammatory response. However, treatment with APE at concentrations of 500, 1000, and 2000 μg/mL significantly reduced the levels of both pro-inflammatory cytokines in a dose-dependent manner, suggesting its ability to suppress inflammation. At a concentration of 2000 μg/mL, APE inhibited TNF-α release, reducing it from 562.83 to 172.83 pg/mL, and decreased IL-6 release from 2576.67 to 235.61 pg/mL on LPS-stimulated control cells. Conversely, APE treatment at 2000 μg/mL significantly upregulated IL-10 secretion, a key anti-inflammatory cytokine involved in immune regulation and inflammation resolution. The increase in IL-10 levels implies that APE not only inhibits pro-inflammatory responses but also promotes anti-inflammatory mechanisms. Similarly, the effects of L-glutathione (GSH) on cytokine secretion were assessed under the same experimental conditions. Treatment with increasing concentrations of GSH significantly suppressed the secretion of TNF-α (Fig. 6A) and IL-6 (Fig. 6B). At 20 mM, GSH reduced TNF-α secretion to approximately 99.5 pg/mL compared to 562.83 pg/mL in the LPS group. IL-6 levels were also markedly reduced from 2576.67 to 1130.86 pg/mL at the highest GSH concentration, reinforcing its anti-inflammatory action. On the contrary, GSH treatment did not significantly alter the levels of IL-10 secretion compared to the LPS group (Fig. 6C). All tested different concentrations of GSH maintained IL-10 at elevated levels similar to the LPS group, with no apparent increase or decrease in expression. Therefore, the GSH primarily acts by suppressing pro-inflammatory cytokine production without modulating anti-inflammatory cytokine IL-10.

Effects of APE on nitric oxide production in LPS-stimulated RAW264.7 cells

The effects of APE on NO production in LPS-stimulated RAW264.7 macrophage cells were examined. The cells were initially stimulated with 1 μg/mL of LPS for 30 min to induce an inflammatory response, followed by treatment with various concentrations of APE (ranging from 62.5 to 2000 μg/mL) for 24 h. The production of NO was subsequently quantified using the Griess assay, which measured nitrite concentration as an indicator of NO release. The results indicated that LPS stimulation significantly increased NO production compared to

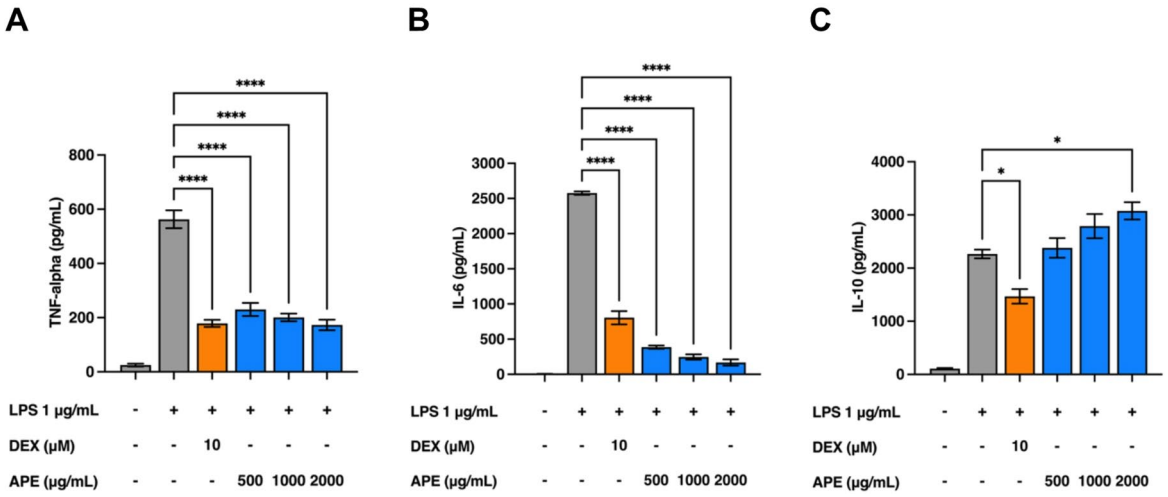

Fig. 5. Effects of APE on the secretion of pro-inflammatory cytokines, including TNF-α (**A**) and IL-6 (**B**), as well as anti-inflammatory cytokine IL-10 (**C**), on LPS-stimulated RAW264.7 cells, with DEX as a reference control. Cells were stimulated with LPS for 30 min and then treated with APE (500–2000 μg/mL) or 10 μM DEX for 24 h. The cytokine levels were measured using an ELISA kit. Results are presented as the cytokine concentration in treated cells. Each value represents the mean ± SEM ($n = 3$). Asterisk indicates significant difference, * ($p \leq 0.05$), ** ($p \leq 0.01$), *** ($p \leq 0.001$) and **** ($p \leq 0.0001$).

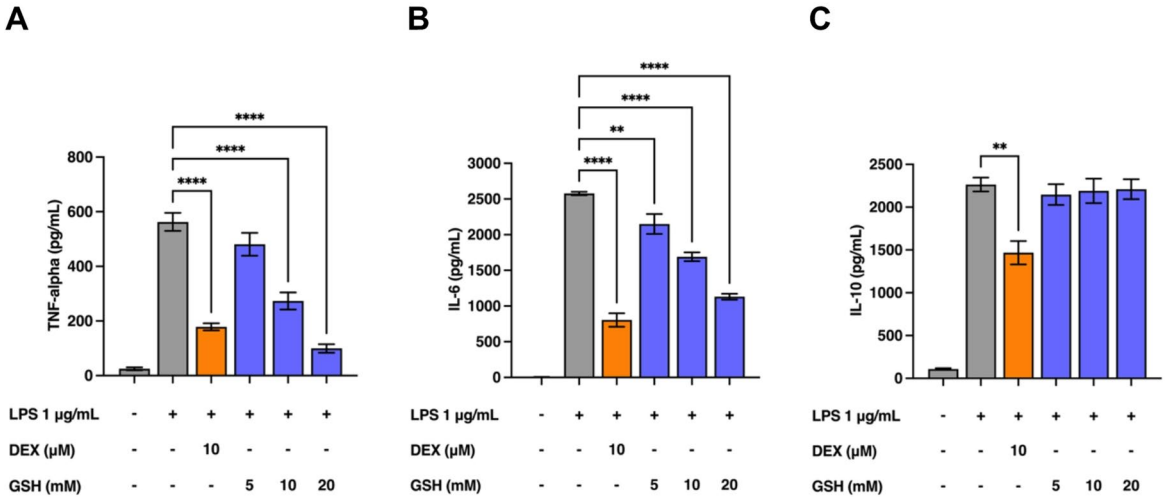

Fig. 6. Effects of GSH on the secretion of pro-inflammatory cytokines, including TNF-α (**A**) and IL-6 (**B**), as well as anti-inflammatory cytokine IL-10 (**C**), on LPS-stimulated RAW264.7 cells, with DEX as a reference control. Cells were stimulated with LPS for 30 min and then treated with GSH (5–20 mM) or 10 μM DEX for 24 h. The cytokine levels were measured using an ELISA kit. Results are presented as the cytokine concentration in treated cells. Each value represents the mean ± SEM ($n = 3$). Asterisk indicates significant difference, * ($p \leq 0.05$), ** ($p \leq 0.01$), *** ($p \leq 0.001$) and **** ($p \leq 0.0001$).

the untreated control group. Treatment with APE led to a dose-dependent reduction in NO levels, with higher concentrations of APE showing a more significant inhibitory effect. At lower concentrations of APE (62.5 and 125 μg/mL), a modest decline in NO levels was observed, while higher concentrations (250, 500, 1000, and 2000 μg/mL) exhibited progressively stronger suppression of NO production, greater than 50%. APE at concentration of 2000 μg/mL could inhibit the nitric oxide production with nearly complete inhibition (Fig. 7A). This dose-dependent inhibition indicates the potent anti-inflammatory potential of APE, likely through the suppression of inducible nitric oxide synthase (iNOS) activity or expression, which is typically upregulated during LPS-stimulated inflammation.

Moreover, 10 nM dexamethasone was used as a reference anti-inflammatory control and 20 mM L-glutathione (GSH) was also applied as a representative antioxidant compound consistent with the major bioactive components identified in APE. The results showed that.

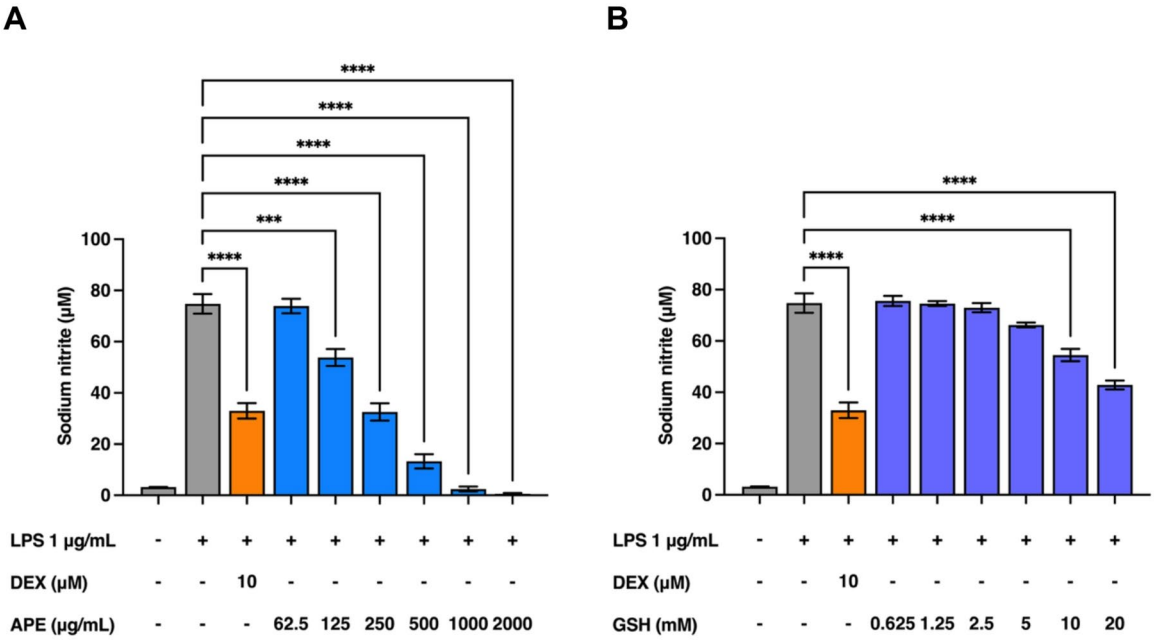

Fig. 7. Effects of APE (**A**) and GSH (**B**) on nitric oxide production in LPS-stimulated RAW264.7 cells, with DEX as a reference control. Cells were stimulated with LPS for 30 min and then treated with APE (62.5–2000 μg/mL), GSH (0.625–20 mM), or 10 μM DEX for 24 h. The amount of nitric oxide produced was determined using the Griess assay. Results are presented as the nitrite concentration, representing nitrogen-based ions released from the treated cell. Each value represents the mean ± SEM ($n = 3$). Asterisk indicates significant difference, * ($p \leq 0.05$), ** ($p \leq 0.01$), *** ($p \leq 0.001$) and **** ($p \leq 0.0001$).

L-glutathione inhibited NO production in a concentration-dependent inhibition (Fig. 7B). High concentrations (5, 10, and 20 mM) of GSH significantly suppressed NO release. At the highest concentration (20 mM), GSH nearly abolished NO production, comparable to the suppression that was observed with dexamethasone (DEX). These findings suggest that GSH may exert anti-inflammatory effects through mechanisms involving the attenuation of iNOS-mediated NO synthesis and consistent with its role as a thiol-based antioxidant.

Effects of APE on intracellular reactive oxygen and nitrogen species (RONS) levels in LPS-stimulated RAW264.7 cells

The impact of APE on intracellular ROS and RNS production in LPS-stimulated RAW264.7 cells was evaluated. Cells were treated with LPS for 30 min to initiate an inflammatory response, followed by treatment with various concentrations of APE (62.5 to 2000 μg/mL) for 24 h. The levels of ROS and RNS were measured using fluorometric assays with DCFH-DA and DAF-FM DA, respectively. The treatment with APE resulted in a dose-dependent decrease in ROS and RNS levels. APE at concentrations greater than 250 μg/mL significantly reduced ROS levels by more than 50% (Fig. 8A) and significantly decreased RNS levels by more than 50% (Fig. 8B). Likewise, the effects of GSH on intracellular ROS and RNS levels were assessed under the same experimental conditions (Fig. 8C and D). Treatment with GSH at concentrations ranging from 0.625 to 20 mM demonstrated a reduction in both ROS and RNS levels. Moreover, GSH at high concentrations of 5, 10, and 20 mM significantly suppressed ROS and RNS generation. GSH (20 mM) reduced ROS to approximately 60% of the LPS-stimulated levels.

The effects of APE on intracellular ROS and RNS were also determined using flow cytometry. Cells were pre-treated with LPS and then exposed to various concentrations of APE. The levels of intracellular ROS and RNS were measured using fluorometric assays with DCFH-DA and DAF-FM DA, respectively. Figure 9A confirms a reduction in intracellular ROS levels, with significant decreases of more than 50% at concentrations greater than 125 μg/mL. Figure 9B shows a parallel decrease in intracellular RNS. The data indicate that APE effectively quenched RNS production in a dose-dependent manner, with significant decreases of more than 50% at concentrations greater than 250 μg/mL. In parallel, the anti-free radical effects of GSH were evaluated to compare its efficacy with APE. As shown in Fig. 9C and D, GSH treatment led to a dose-dependent suppression of both intracellular ROS and RNS levels in LPS-stimulated RAW264.7 cells. Specifically, ROS levels were significantly reduced at concentrations ≥ 5 mM. The most prominent reduction observed at 20 mM, bringing ROS levels down to nearly 40% of LPS-induced levels. Similarly, RNS levels showed a significant decline at higher GSH concentrations, particularly at 20 mM, where RNS levels decreased to 65%.

The flow cytometry histograms (Fig. 10) show the three treatments in each experiment: the control group, which consisted of untreated cells, the LPS-stimulated group, in which cells were exposed to LPS to induce oxidative stress, and the APE treated group. The fluorescence intensity of DCF was measured as an indicator of ROS levels, while the fluorescence intensity of DAF-FM-T was used to assess RNS levels. In the control

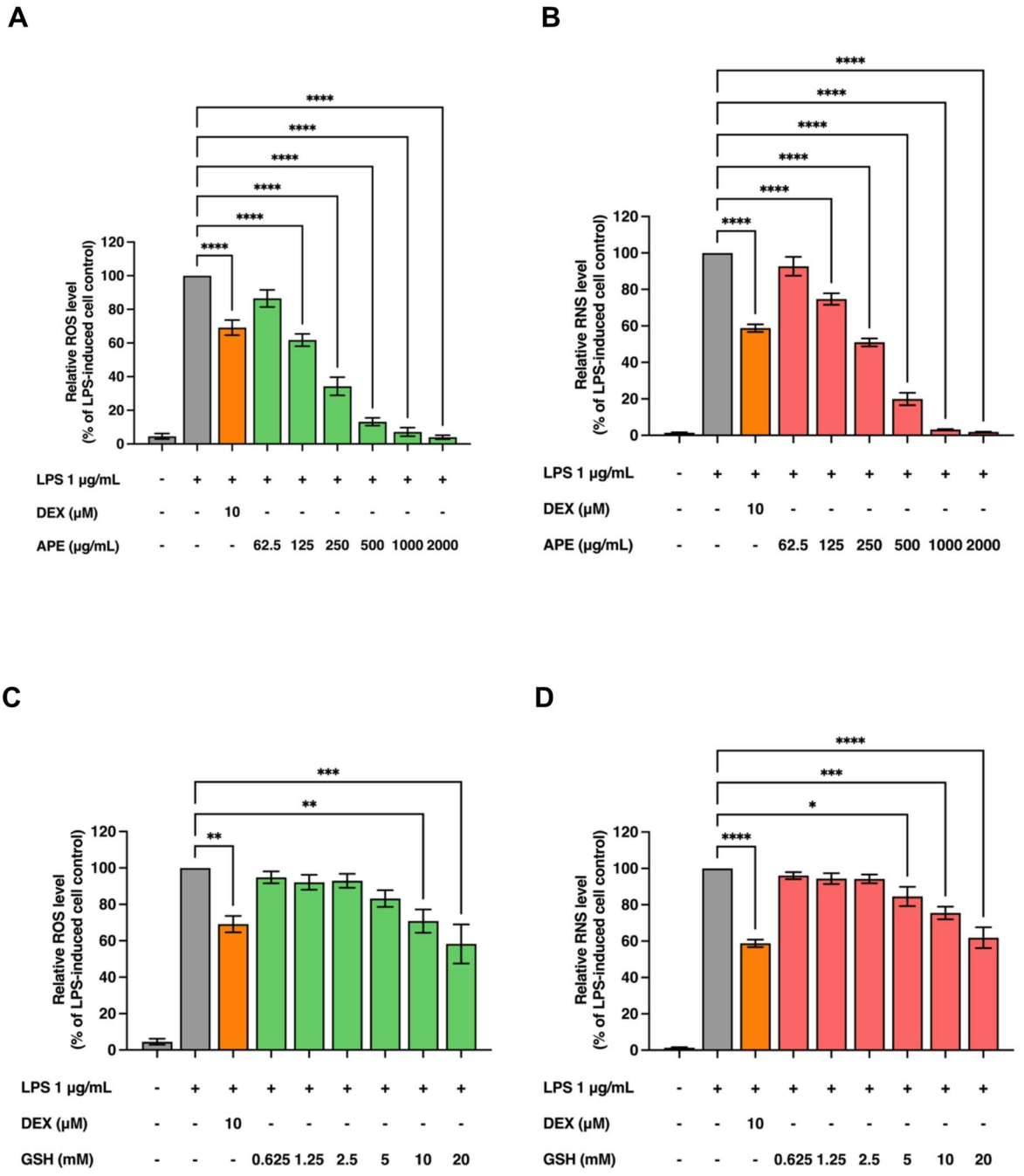

Fig. 8. Effects of APE (**A**) and (**B**) and GSH (**C**) and (**D**) on intracellular ROS and RNS production in LPS-stimulated RAW264.7 cells using DEX as a reference control. Cells were stimulated with LPS for 30 min and then treated with APE (62.5–2000 μg/mL), GSH (0.625–20 mM), or 10 μM DEX for 24 h. The level of ROS and RNS were determined using fluorometric assay with a DCFH-DA and DAF-FM DA, respectively. Results are expressed as the relative RONS levels compared to LPS-stimulated cells group. Each value represents the mean ± SEM ($n = 3$). Asterisk indicates significant difference, * ($p \leq 0.05$), ** ($p \leq 0.01$), *** ($p \leq 0.001$) and **** ($p \leq 0.0001$).

group, ROS levels were minimal, with cells exhibiting DCF fluorescence, indicating a baseline level of oxidative stress. However, LPS stimulation significantly increased ROS levels, as evidenced by a dramatic rise in DCF fluorescence to 93.49%. The APE treatment significantly reduced ROS levels, as the proportion of DCF-positive cells dropped to 23.30%. Similarly, RNS levels exhibited a comparable trend. In the control group, nitrosative stress was detected, with minimal levels. However, LPS stimulation resulted in a substantial increase in RNS production, with 90.42% of cells displaying fluorescence. The APE treatment significantly reduced RNS levels, with the percentage of DAF-FM-T positive cells decreasing to 24.25%.

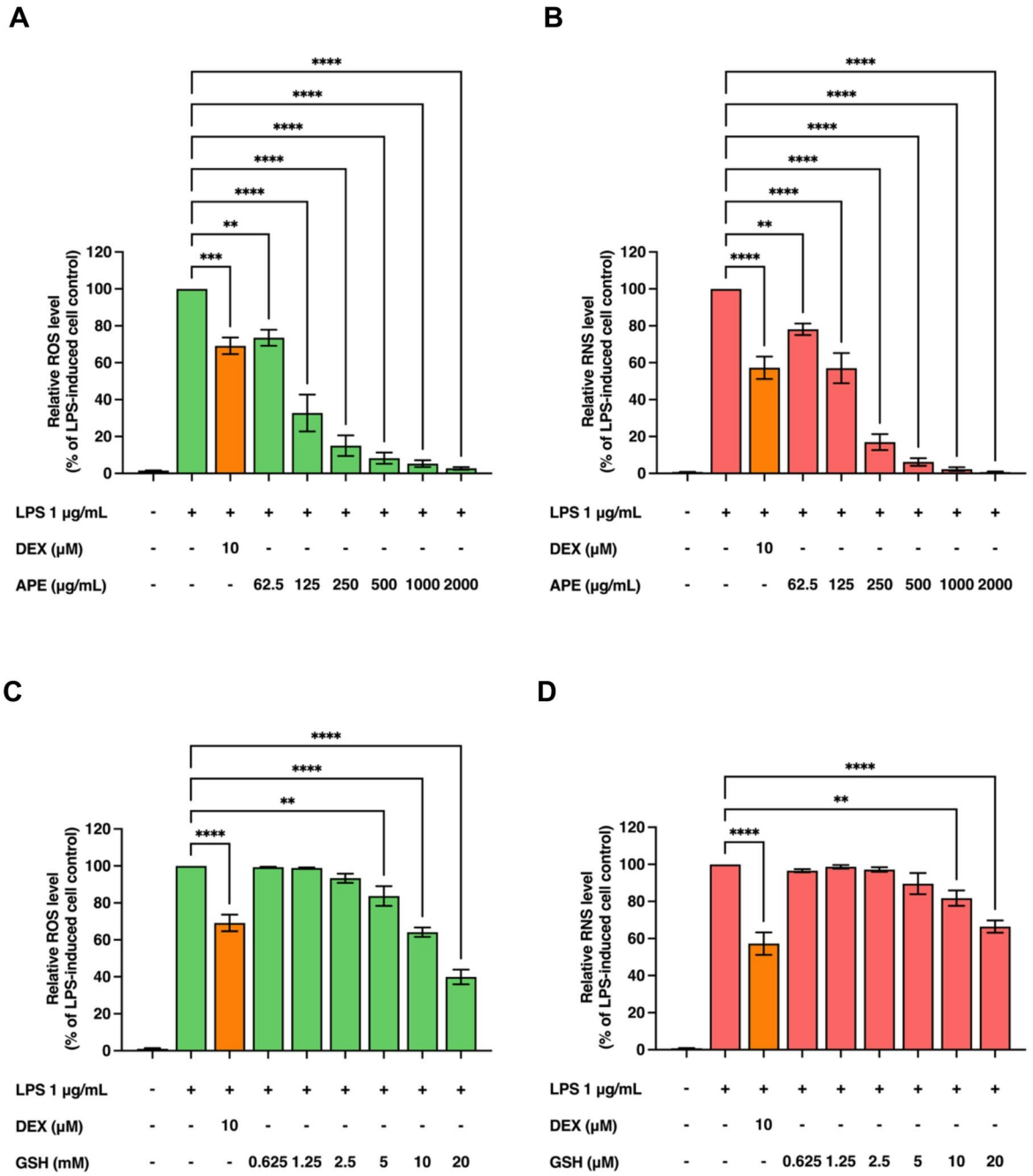

Fig. 9. Effects of APE (**A**) and (**B**) and GSH (**C**) and (**D**) on intracellular ROS and RNS generation in LPS-stimulated RAW264.7 cells using DEX as a reference control. Cells were stimulated with LPS for 30 min and then treated with APE (62.5–2000 µg/mL), GSH (0.625–20 mM), or 10 µM DEX for 24 h. The level of ROS and RNS were evaluated by flow cytometry using DCFH-DA and DAF-FM DA, respectively. Results are expressed as the relative RONS level compared to LPS-stimulated cells group. Each value represents the mean ± SEM ($n = 3$). Asterisk indicates significant difference, * ($p \leq 0.05$), ** ($p \leq 0.01$), *** ($p \leq 0.001$) and **** ($p \leq 0.0001$).

Effects of APE on oxidative stress in LPS-stimulated RAW264.7 cells

The effect of APE on oxidative stress in LPS-stimulated RAW264.7 cells was evaluated. Cells were treated with LPS for 30 min to initiate an inflammatory response, followed by treatment with various concentrations of APE (500 to 2000 µg/mL) and GSH (5 to 10 mM) for 24 h. The oxidative stress marker, including malondialdehyde (MDA) and glutathione redox status were measured using colorimetric assays with TBARS assay and Ellman's assay, respectively. On MDA levels, treatment with LPS significantly increased MDA levels compared to control ($p < 0.01$), indicating elevated oxidative stress. The treatment with both of APE (Fig. 11A) and GSH (Fig. 11B) significantly reduced MDA levels. Specifically, APE at concentrations of 500, 1000, and 2000 mg/mL significantly decreased MDA levels compared to LPS-induced cell group.

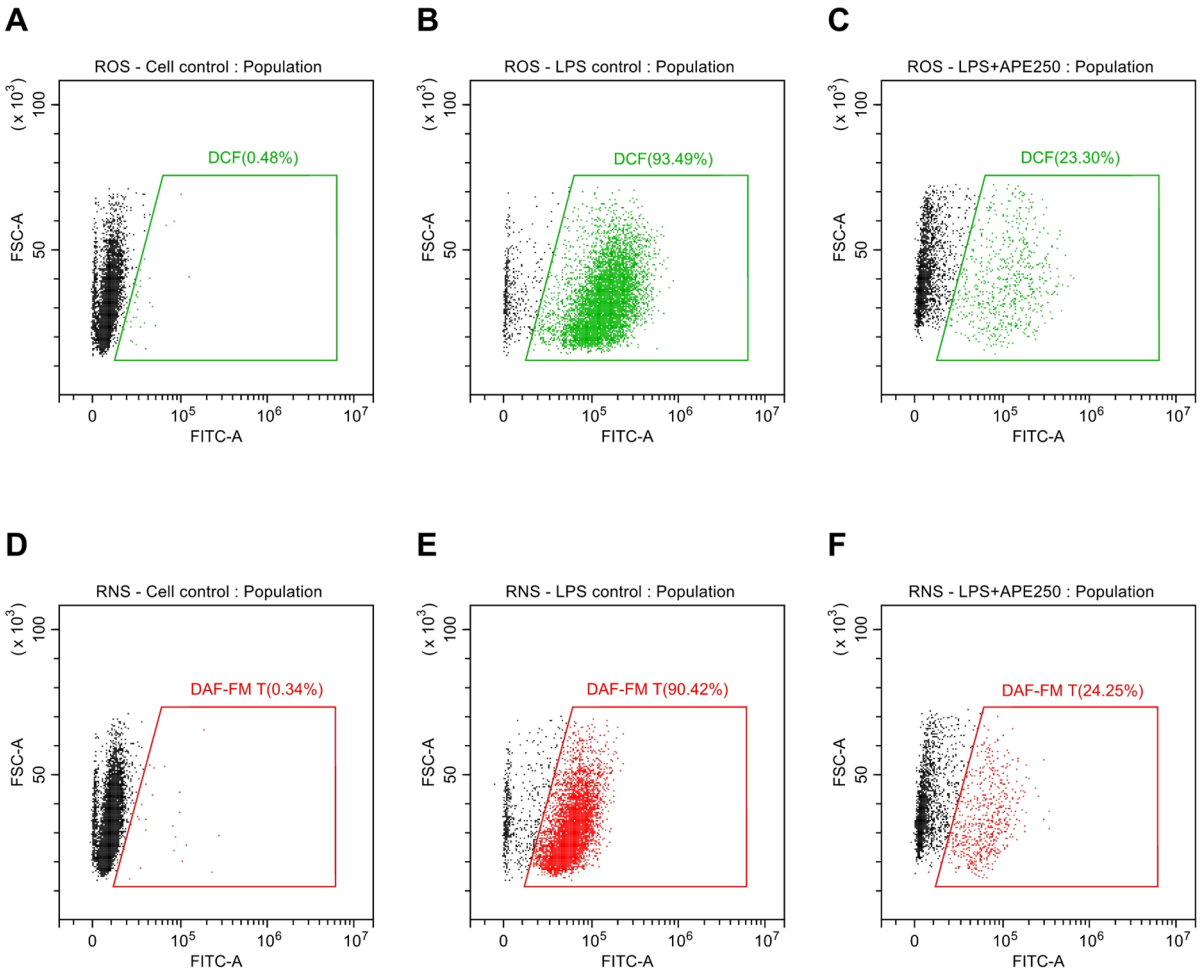

Fig. 10. Assessment of intracellular ROS (**A**)–(**C**) and RNS (**D**)–(**F**) using flow cytometry. Flow cytometry data are presented as dot plot histograms with cell population gated using forward scatter (FSC-A) versus fluorescence intensity in the fluorescein isothiocyanate (FITC)-A channel. Experimental groups included untreated control cells (**A**), (**D**), LPS-stimulated cells (**B**), (**E**), and LPS-stimulated cells treated with APE at concentration of 250 µg/mL (**C**), (**F**).

Likewise, GSH at 5, 10, and 20 mM significant reduced MDA, suggesting its potent antioxidant activity. These data indicated that both APE and GSH effectively protected LPS-induced lipid peroxidation. Panels B and E of Fig. 11 show the concentrations of total glutathione (GSHt) and oxidized glutathione (GSSG). LPS treatment led to a slight decrease in GSH and an increase in GSSG levels, indicating oxidative imbalance. Treatment with APE helped restore GSH levels and reduced GSSG accumulation, particularly at higher doses. The glutathione redox status was calculated from GSH/GSSG ratio. LPS treatment significantly decreased this ratio, confirming oxidative stress. APE significantly improved the GSH/GSSG ratio in a dose-dependent manner. APE at 1000 and 2000 mg/mL, and GSH at all tested doses (5, 10, 20 mM), significantly improved the redox ratio, indicating their capacity to rebalance oxidative stress. In contrast, GSH treatment did not significantly improve the GSH/GSSG ratio at any of the tested doses, indicating that exogenous GSH alone may be insufficient to restore redox balance under the given experimental conditions.

Discussion

Arthrospira (*Spirulina*) *platensis* extract (APE) contains a wide array of bioactive compounds with potential therapeutic and nutritional properties. The phytochemical and metabolite profiling of APE revealed the presence of various bioactive compounds that may contribute to its biological activities. The high protein content highlights the nutritional potential of APE. The phycobiliproteins, especially phycocyanin and allophycocyanin being the major components. These pigments are known for their strong antioxidant, anti-inflammatory, and light-harvesting properties, particularly in cyanobacteria, which suggests their functional relevance in APE[48–50]. The detection of L-glutathione and total phenolic compounds further supports the antioxidant capacity of APE. L-glutathione plays a crucial role in cellular redox homeostasis, while phenolic compounds are secondary metabolite for their free radical scavenging activities[51,52]. In agreement with the colorimetric assays, LC–MS analysis confirmed the presence of several key metabolites with antioxidant and anti-inflammatory relevance.

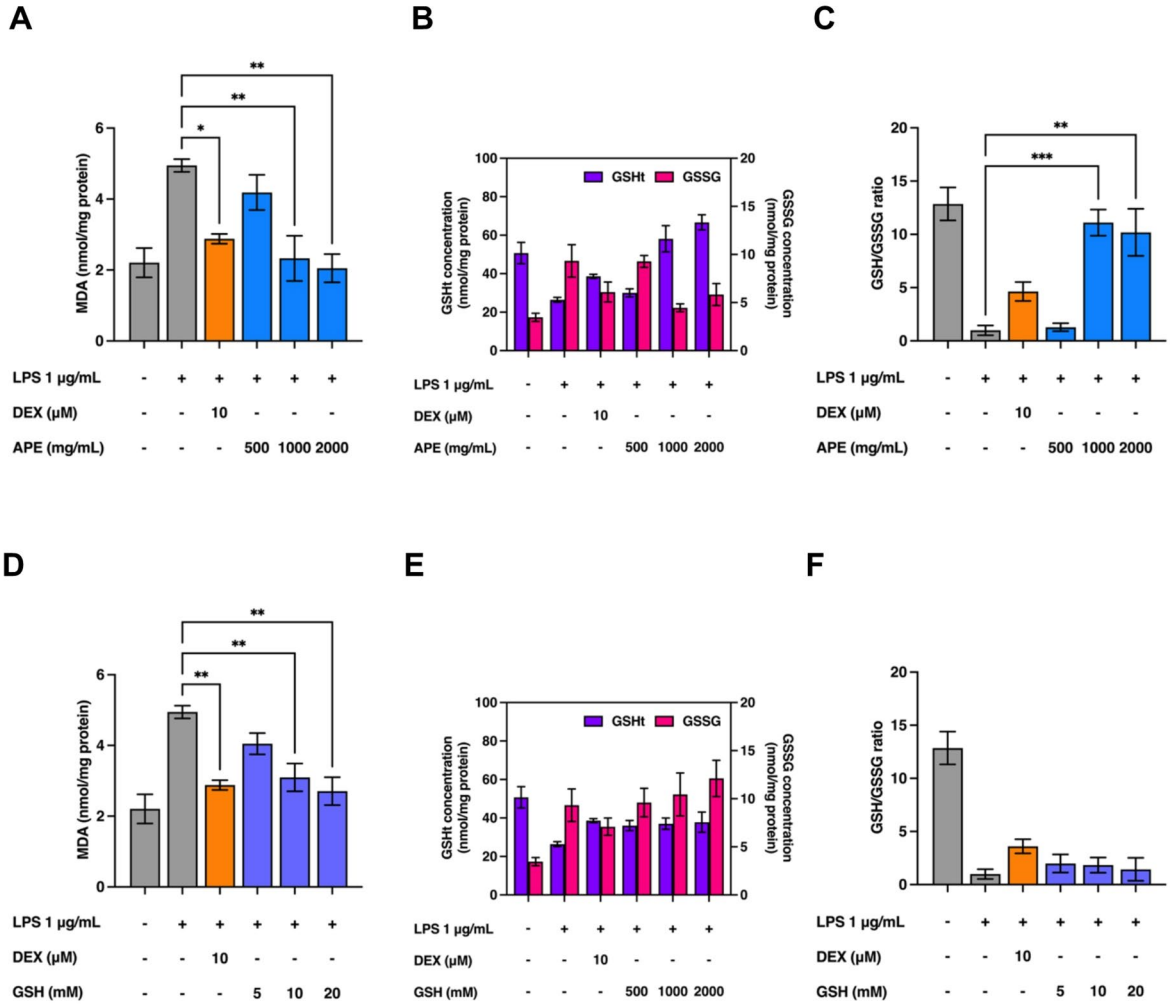

Fig. 11. Effects of APE (**A**), (**B**) and (**C**) and GSH (**D**), (**E**), and (**F**) on oxidative stress in LPS-stimulated RAW264.7 cells using DEX as a reference control. Cells were stimulated with LPS for 30 min and then treated with APE (500–2000 µg/mL), GSH (5–20 mM), or 10 µM DEX for 24 h. The oxidative stress marker, MDA (A and D) and glutathione redox status (B, C, E, and F) were measured using colorimetric assays. Results are expressed as the relative RONS levels compared to LPS-stimulated cells group. Each value represents the mean ± SEM ($n = 3$). Asterisk indicates significant difference, * ($p \leq 0.05$), ** ($p \leq 0.01$), *** ($p \leq 0.001$) and **** ($p \leq 0.0001$).

Notably, glutathione and L-(+)-ergothioneine were identified, both of which are recognized for their roles in protecting cells against oxidative stress. The presence of L-pyroglutamic acid, a glutathione-related metabolite, further strengthens this observation. The identification of purine bases such as adenine, guanine, and hypoxanthine suggests the presence of nucleotide metabolism-related pathways in APE. These compounds are not only involved in nucleic acid synthesis but also have roles in cellular signalling and immune modulation[53,54]. In addition, amino acids such as phenylalanine, valine, leucine, and norvaline were identified, reflecting the protein-rich nature of the extract and its potential nutritional benefits.

These findings supported previous studies on other cyanobacterial species that also demonstrated the presence of diverse bioactive compounds with potential health benefits. For instance, *Anabaena variabilis* and *S. platensis* collected in Egypt showed varied phytochemical profiles, with GC–MS analysis revealing 37 and 7 bioactive compounds, respectively. The relative abundance of compounds consisting fatty acid methyl esters and heterocyclic compounds[55]. Other study of freshwater cyanobacterium, *Nostoc muscorum* demonstrated a wide spectrum of bioactive molecules, including sugars, oligosaccharides, ω-3 and ω-6 fatty acids, amino acids, pigments, and mycosporin-like peptides[56]. Moreover, LC-ESI-QTOF-MS/MS analysis of *Nostoc* sp. AARL C008 methanolic extract identified up to 83 phenolic compounds, with p-coumaric acid being the most abundant[57]. Thus, this observation highlights the significant contribution of phenolic compounds to the antioxidant potential of cyanobacterial extracts. Furthermore, extraction of *S. platensis* using water can obtain polysaccharides from their cellular matrix[58]. Notably, sulphated polysaccharides, especially calcium spirulan, have been recognized as bioactive macromolecules with diverse pharmacological properties, including immunomodulatory, antiviral, and antioxidant activities. However, efficient extraction of polysaccharide usually requires alkaline solvents or

elevated temperature (80–100 °C) to enhance yield. In contrast, extraction at lower temperatures is feasible but typically demands an extended processing period, often ranging from several hours to days[59–61].

Previous studies have consistently demonstrated the immunomodulatory potential of *Arthrospira* (*Spirulina*) *platensis* polysaccharide. The polysaccharide extract exhibited very low cytotoxicity toward RAW264.7 macrophages, with cell viability remaining above 80% even at concentrations up to 2000 µg/mL. Similarly, the polysaccharides extracted at 400 µg/mL showed no cytotoxic effects on mouse dermal fibroblast cell line (MDF), indicating a broad safety profile across different immune cell types. Notably, low-molecular weight polysaccharide fractions have been shown to stimulate mouse spleen lymphocyte proliferation and enhance the phagocytic activity of RAW264.7 macrophages. The polysaccharide has also been reported to increase the production of nitric oxide, TNF-α, and IL-6 in a concentration-dependent manner, whereas lower concentration (50 µg/mL) had no significant effect on nitric oxide production[62].

However, our result indicated that polysaccharides accounted for only approximately 17% of the total composition in APE, which may contribute to the slightly stimulate cytokine responses in cell culture. Therefore, the biological effects that detected in this study are likely to reflect the combined action of polysaccharides and other coexisting bioactive compounds, rather than the immunomodulatory potential of polysaccharides alone[62,63]. These findings indicate that the coexistence of proteins, pigments, amino acids, phenolic compounds, and polysaccharides contributes to the multifunctional nutritional and therapeutic potential of aqueous *S. platensis* extract[64,65]. However, some bioactive compounds within the extract, particularly phycocyanin and glutathione, exhibit relatively low stability. Phycocyanin is highly heat-sensitive, whereas glutathione readily undergoes redox reactions upon exposure to oxygen[66,67]. Thus, proper storage conditions are essential to preserve their biological activity. To ensure stability, the extract should be maintained in powdered form at –20 °C under dry and light-protected conditions. Following reconstitution, it is advisable to aliquot the extract into multiple tubes and avoid repeated freeze–thaw cycles to retain its stability and functional integrity.

The APE has been recognized for its bioactive properties, particularly its anti-inflammatory and antioxidant potential. To assess its safety for therapeutic use, its cytotoxicity was evaluated in RAW264.7 and human leukocytes, including peripheral blood mononuclear (PBMCs) and polymorphonuclear leukocytes (PMNs) cells. The cytotoxicity assay results revealed that APE did not exhibit significant cytotoxic effects on RAW264.7 cells at concentrations up to 2000 µg/mL. This finding supports the safety of APE at therapeutic doses, making it a promising candidate for further exploration in anti-inflammatory and antioxidant therapies. The low cytotoxicity of APE suggests that the extract exerts its protective effects without compromising cellular integrity, a critical consideration for potential pharmacological applications.

Several cyanobacterial extracts have demonstrated low toxicity to cell culture. Methanolic extracts from cyanobacteria such as *Cylindrospermopsis raciborskii*, *Aphanizomenon gracile*, *Microcystis ichtyoblabe*, *Planktothrix agardhii*, and *Limnothrix redekei* have shown low toxicity to the human hepatoblastoma cell line (Hep G2) after 24 h of exposure. All extracts at a concentration of 2 mg/mL exhibited low cytotoxicity to HepG2 cells, with cell viability remaining above 50%[68]. The cytotoxicity of bioactive compound extracts derived from *Arthrospira* sp. has also been studied. Phycocyanobilin derived from *A. maxima* at a concentration of 1000 µg/mL showed low toxicity in the human skin fibroblast cell line (CCD-986sk), with cell viability remaining greater than 50% after 24 h of treatment. Additionally, the aqueous extract from *A. maxima* also exhibited low toxicity in the human lung carcinoma cell line (H460)[69,70]. Bioactive compounds derived from *S. platensis, Nostoc* spp., and *Anabaena* spp. have been reported to exhibit low cytotoxicity in cultured cells. These extracts contain bioactive compounds, including phycocyanin, polysaccharides, and secondary metabolites, which have anti-inflammatory and antioxidant effects, and demonstrated high biocompatibility with mammalian cells[71,72].

Regarding the anti-inflammatory activities of APE, the results demonstrated that APE significantly reduces NO production in LPS-stimulated RAW264.7 macrophage cells in a dose-dependent manner. LPS markedly increased NO levels in RAW264.7 cells, indicating an inflammatory response. However, APE treatment effectively attenuated NO production. At higher concentrations (500–2000 µg/mL), NO levels were reduced to near baseline levels, similar to the control group, suggesting that APE possesses potent anti-inflammatory properties. Moreover, APE was found to suppress gene and protein expression of inducible nitric oxide synthase (iNOS). The reduction in NO levels aligned with previous studies on natural extracts rich in polyphenols and flavonoids, which have been shown to inhibit iNOS expression and mitigate inflammation through the downregulation of NF-κB signaling[73,74].

Various compounds derived from cyanobacteria have demonstrated significant anti-inflammatory potential. For instance, the extracts of *Arthrospira* (*Spirulina*) sp. have demonstrated significant potential in modulating cytokine imbalance and reducing inflammation in various inflammatory models. The extract of *S. maxima* extract, obtained through a two-phase method using 70% ethanol, suppressed LPS-stimulated upregulation of pro-inflammatory cytokines such as TNF-α, IL-1β, IL-12, and IL-18 in RAW264.7 cells. Additionally, the extract inhibited LPS-induced phosphorylation of extracellular signal-regulated kinase (ERK) in RAW264.7 cells, attenuating the generation of ERK1-induced reactive oxygen species (ROS) and leading to decreased NF-κB expression[75]. The administration of *S. maxima* in Sprague–Dawley rats significantly reduced pro-inflammatory cytokines such as TNF-α, IL-1β, and IL-6, as well as the inflammatory transcription factor.

NF-κB in gingival tissue. In contrast, *S. maxima* increased the production of anti-inflammatory cytokine IL-4 by T-helper type 2 (Th2) cells[76]. Furthermore, the administration of

S. platensis has been shown to prevent methotrexate (MTX)-induced neurotoxicity in Wistar Albino rats, reducing the levels of IL-1β, IL-6, and TNF-α in the brain tissue of MTX-induced rats[77]. Apart from cyanobacteria, sulfated polysaccharides derived from red microalgae exhibit anti-inflammatory properties, particularly in skin inflammation, by recruiting leukocytes from capillary blood to the inflammation site, which involves adhesion and chemotaxis[78]. The study demonstrated that these polysaccharides inhibited polymorphonuclear leukocyte

(PMN) migration toward chemoattractant molecules and partially blocked PMN adhesion to endothelial cells *in vitro*.

Polysaccharides from microalgae have been found to exhibit pharmacological activities, including not only anti-inflammatory activity but also immunomodulatory effects. The exopolysaccharide extract from *Tribonema* sp. stimulated macrophage cell activation, leading to the upregulating of pro-inflammatory cytokines, including TNF-α, IL-6, and IL-10. Similarly, the exopolysaccharide derived from *Nostoc* sp. induced the release of prostaglandins E2 (PGE2) and NO by upregulating the gene expression of *COX-2* and *iNOS*, respectively[79]. The expression of iNOS and COX-2 genes in macrophages is largely regulated by transcriptional activation. These findings suggest that exopolysaccharide extracts from cyanobacteria enhance the early activation of the innate immune response, primarily through the upregulation of key inflammatory mediators, which play a pivotal role in the initiation of immune defense mechanisms[80,81]. By stimulating macrophage activity and promoting the release of immune modulators, this exopolysaccharide holds potential as a novel immune modulator that is capable of enhancing immune responses and possibly serving as a therapeutic agent for inflammatory disorders[82].

Comparing to reference control, dexamethasone (DEX) potently inhibits NF-κB activation, proinflammatory cytokines, and COX-2 expression in RAW 264.7. At low concentration of DEX (approximately 10 nM) demonstrated the ability to inhibit granulocyte–macrophage colony-stimulating factor (GM-CSF) and suppress NF-κB expression. At higher concentration levels (approximately 10 μM), DEX blocks LPS induced NF-κB/AP1 signalling and halting IL-1β transcription. Thus, DEX (10 μM) demonstrates anti-inflammatory actions and protects oxidative stress. However, it may also induce adverse effects like apoptosis and immune modulation depending on exposure duration[83,84].

The study also investigated the effects of APE on intracellular ROS and RNS levels in LPS-stimulated macrophages. Both ROS and RNS production significantly increased after LPS stimulation, indicating oxidative stress induced by inflammatory activation. Treatment with APE effectively reduced these elevated levels in a concentration-dependent manner. At higher concentrations (500–2000 μg/mL), the reduction in ROS and RNS levels was particularly pronounced, suggesting that APE exerts a dual antioxidant and anti-inflammatory effect. These findings imply that APE may enhance the activity of antioxidant defense systems, such as the Nrf2/HO-1 pathway, or directly scavenge free radicals[85,86,87].

Studies on crude extracts from cyanobacteria, including *Nostoc* sp., *Leptolyngbya protospira, Nodularia spumigena,* and *Phormidiochaete* sp. have shown significant DPPH scavenging capacity[88]. Natural compounds derived from cyanobacteria, such as *Anabaena* sp., *Nodularia* sp., *Nostoc* sp., and *S. platensis,* have also demonstrated strong antioxidant activity in various antioxidant assays, including DPPH free radical scavenging, reducing power, and metal chelating activity[89]. Although cyanobacteria rely on photosynthesis for energy production, they must possess robust antioxidant defence mechanisms to mitigate the generation of reactive oxygen and nitrogen species (RONS) within their cells. The continuous exposure to high-intensity light and oxygen-rich environments during photosynthesis makes them particularly susceptible to oxidative stress. To counteract this, cyanobacteria have evolved efficient antioxidant systems, including enzymatic antioxidants such as superoxide dismutase (SOD), catalase (CAT), and peroxidases, as well as non-enzymatic antioxidants, e.g., phycocyanin, carotenoids, and vitamin E. These protective compounds play a crucial role in maintaining cellular homeostasis, preventing oxidative damage to essential biomolecules, and ensuring the stability of photosynthetic machinery, thus supporting the survival and functionality of cyanobacterial cells in diverse environmental conditions[90,91,92].

L-Glutathione (GSH) is a key intracellular antioxidant that plays a central role in modulating oxidative stress and inflammation. Studies have shown that GSH can suppress the expression of pro-inflammatory cytokines such as IL-1β, IL-6, and TNF-α by reducing ROS levels and modulating the AKT/PI3K/PTEN signalling pathway[93]. In joint-related inflammation models, GSH supplementation improved antioxidant capacity and downregulated inflammatory gene expression in synoviocytes, and the effects were concentration-dependent[94]. In some metabolic diseases or infection disease, the reduced GSH levels are strongly associated with heightened oxidative stress and cytokine imbalance, indicating the protective role of GSH in these conditions[95,96].

The present findings demonstrate that both APE and GSH also exhibit protective effects against LPS-induced oxidative stress in RAW264.7 macrophages. Treatment with APE at 500–2000 μg/mL and GSH at 5–20 mM significantly reduced MDA levels, indicating potent inhibition of lipid peroxidation. APE decreased MDA levels and improved the GSH/GSSG ratio. This interpretation is supported by other studies examining the biological effects of *A. platensis*. For instance, Spirulina extract was shown to reduce ROS and MDA levels in A549 lung cancer cells and to disrupt cancer cell proliferation by inducing cell cycle arrest. Furthermore, an aqueous extract of *S. maxima* demonstrated neuroprotective properties by reducing oxidative stress markers such as ROS and intracellular calcium, preserving mitochondrial membrane integrity, and elevating reduced glutathione levels[97,98]. This observation suggests that the extract not only counters oxidative damage but may also modulate cellular signalling pathways associated with cell growth and survival. Additionally, Spirulina was found to reduce MDA accumulation and preserved renal function in rats treated with cyclosporine A, indicating its protective effect against drug-induced oxidative stress and nephrotoxicity. In broiler chickens, dietary supplementation with *A. platensis* enhanced antioxidant enzyme activities, including glutathione peroxidase, and improved nutrient absorption and gut health, further reinforcing its systemic antioxidant capacity[99,100].

Taken together, these findings highlight that the protective effect of APE observed in the present study may be attributed to a combination of its constituent bioactive compounds, including phycocyanin, phenolics, glutathione, and amino acids. The synergistic action of these compounds likely contributes to both direct free radical scavenging and restoration of the cellular antioxidant system. Unlike single-compound treatments such as pure GSH, the multifaceted composition of APE may offer broader biological benefits, including modulation of redox-sensitive signalling pathways and enhancement of endogenous antioxidant defence. Therefore, *A.*

platensis extract holds promise as a natural therapeutic agent for mitigating inflammation-associated oxidative stress[101,102].

In the context of LPS-stimulated RAW264.7 macrophages, studies have demonstrated that phycocyanin, phenolic compound and L-glutathione from *A. platensis* significantly reduces NO production, similar to the effects observed in the current study[38]. This reduction is primarily attributed to the downregulation of iNOS and inhibition of NF-κB signalling pathways. Furthermore, the antioxidant capacity of APE is enhanced by its ability to scavenge free radicals and modulate the Nrf2/HO-1 pathway, as evidenced by its concentration-dependent attenuation of ROS and RNS levels[87]. Although *A. platensis* has long been used as a food supplement, further investigation is needed to explore its therapeutic potential, mechanisms of action, and both short-term and long-term effects[24]. Since most conclusions in this study are based on in vitro experiments, future research should prioritize animal models and large-scale clinical trials in human cohorts to validate these findings. Nevertheless, *A. platensis* holds significant promise in the nutraceutical, cosmeceutical, and pharmaceutical industries[103].

Conclusion

Arthrospira platensis has extensive nutritional and therapeutic applications due to its bioactive components, including phycocyanin, β-carotene, and polysaccharides. This extract also contains antioxidant-related compounds such as glutathione and ergothioneine. These components play crucial roles in combating oxidative stress, reducing inflammation, and modulating immune responses. *A. platensis* inhibited the secretion of pro-inflammatory mediators such as TNF-α and IL-6, while also upregulated the secretion of IL-10, an anti-inflammatory cytokine. Furthermore, *A. platensis* regulated the inflammation by suppressing the expression of the *iNOS* gene and protein, leading to the inhibition of NO secretion in LPS-stimulated RAW264.7 cells. Additionally, *A. platensis* demonstrated strong potential in protecting cells from oxidative stress by reducing of intracellular RONS generation in LPS-stimulated RAW264.7 cells. The *A. platensis* also attenuated oxidative stress by reducing MDA levels associated with lipid peroxidation and restoring glutathione status. These findings demonstrated the potential of *A. platensis* extract as a functional ingredient for anti- inflammation and ani-free radical effects.

Data availability

The data presented in this study are available on request from the corresponding author.

Received: 17 April 2025; Accepted: 3 November 2025
Published online: 08 December 2025

References

1. Chen, L. et al. Inflammatory responses and inflammation-associated diseases in organs. *Oncotarget* **9**, 7204–7218 (2017).
2. Netea, M. G. et al. A guiding map for inflammation. *Nat. Immunol.* **18**, 826–831 (2017).
3. Soares, C. L. R. et al. Biochemical aspects of the inflammatory process: A narrative review. *Biomed. Pharmacother.* **168**, 115764 (2023).
4. de Nooijer, A. H., Pickkers, P., Netea, M. G. & Kox, M. Inflammatory biomarkers to predict the prognosis of acute bacterial and viral infections. *J. Crit. Care.* **78**, 154360 (2023).
5. Rodríguez-Morales, P. & Franklin, R. A. Macrophage phenotypes and functions: Resolving inflammation and restoring homeostasis. *Trends Immunol.* **44**, 986–998 (2023).
6. Suzuki, K. Chronic inflammation as an immunological abnormality and effectiveness of exercise. *Biomolecules* **9**, 223 (2019).
7. Furman, D. et al. Chronic inflammation in the etiology of disease across the life span. *Nat. Med.* **25**, 1822–1832 (2019).
8. McInnes, I. B. & Gravallese, E. M. Immune-mediated inflammatory disease therapeutics: Past, present and future. *Nat. Rev. Immunol.* **21**, 680–686 (2021).
9. Hussain, T. et al. Oxidative stress and inflammation: What polyphenols can do for us?. *Oxid. Med. Cell Longev.* **2016**, 7432797 (2016).
10. Zuo, L. et al. Inflammaging and oxidative stress in human diseases: from molecular mechanisms to novel treatments. *Int. J. Mol. Sci.* **20**, 4472 (2019).
11. Mittal, M., Siddiqui, M. R., Tran, K., Reddy, S. P. & Malik, A. B. Reactive oxygen species in inflammation and tissue injury. *Antioxid. Redox Signal.* **20**, 1126–1167 (2014).
12. Sies, H. et al. Defining roles of specific reactive oxygen species (ROS) in cell biology and physiology. *Nat. Rev. Mol. Cell Biol.* **23**, 499–515 (2022).
13. Yu, W. et al. Reactive oxygen species bridge the gap between chronic inflammation and tumor development. *Oxid. Med. Cell. Longev.* **2022**, 2606928 (2022).
14. Bindu, S., Mazumder, S. & Bandyopadhyay, U. Non-steroidal anti-inflammatory drugs (NSAIDs) and organ damage: A current perspective. *Biochem. Pharmacol.* **180**, 114147 (2020).
15. Wood, H. Anti-inflammatory drugs could cause chronic pain. *Nat Rev Neurol.* **18**, 382 (2022).
16. Azab, A., Nassar, A. & Azab, A. N. Anti-inflammatory activity of natural products. *Molecules* **21**, 1321 (2016).
17. De Ravi, M. S. L., Azharuddin, S. D. & Paul, S. F. Paul SF The beneficial effects of spirulina focusing on its immunomodulatory and antioxidant properties. *Nutr. Dietary Suppl.* **2**, 73–83 (2010).
18. Bortolini, D. G. et al. Functional properties of bioactive compounds from *Spirulina* spp.: current status and future trends. *Food Chem. Mol. Sci.* **5**, 100134 (2022).
19. Calella, P. et al. Antioxidant, anti-inflammatory and immunomodulatory effects of spirulina in exercise and sport: a systematic review. *Front. Nutr.* **9**, 1048258 (2022).
20. Muñoz-Ochoa, M., Murillo-Álvarez, J. I., Zermeño-Cervantes, L. A., Martínez-Díaz, S. & Rodríguez-Riosmena, R. Screening of extracts of algae from Baja California Sur, Mexico as reversers of the antibiotic resistance of some pathogenic bacteria. *Eur. Rev. Med. Pharmacol. Sci.* **14**, 739–747 (2010).
21. Mise, T., Ueda, M. & Yasumoto, T. Production of fucoxanthin-rich powder from *Cladosiphon okamuranus*. *Adv. J. Food Sci. Technol.* **3**, 73–76 (2011).
22. Antony, T., Chakraborty, K. & Joy, M. Antioxidative dolabellanes and dolastanes from brown seaweed *Padina tetrastromatica* as dual inhibitors of starch digestive enzymes. *Nat. Prod. Res.* **35**, 614–626 (2021).
23. Yang, D. J. et al. Suppressive effect of carotenoid extract of Dunaliella salina alga on production of LPS-stimulated pro-inflammatory mediators in RAW264.7 cells via NF-κB and JNK inactivation. *J. Funct. Foods.* **5**, 607–615 (2013).

24. Wu, Q. et al. The antioxidant, immunomodulatory, and anti-inflammatory activities of *Spirulina*: an overview. *Arch Toxicol.* **90**, 1817–1840 (2016).
25. Finamore, A., Palmery, M., Bensehaila, S. & Peluso, I. Antioxidant, immunomodulating, and microbial-modulating activities of the stainable and ecofriendly *Spirulina*. *Oxid Med Cell Longev.* **2017**, 3247528 (2017).
26. Bax, C. E. et al. Herbal supplement Spirulina stimulates inflammatory cytokine production in patients with dermatomyositis *in vitro*. *iScience.* **26**, 108355 (2023).
27. Marjanović, B. et al. Bioactive compounds from Spirulina spp.—nutritional value, extraction, and application in food industry. *Separations.* **11**(9), 257 (2024).
28. Cruz-Martínez, L. C. et al. Growth and composition of *Arthrospira* (*Spirulina*) *platensis* in a tubular photobioreactor using ammonium nitrate as the nitrogen source in a fed-batch process. *Braz. J. Chem. Eng.* **32**, 347–356 (2015).
29. Chaiklahan, R., Chirasuwan, N., Loha, V., Tia, S. & Bunnag, B. Separation and purification of phycocyanin from *Spirulina* sp. using a membrane process. *Bioresour. Technol.* **102**, 7159–7164 (2011).
30. Hong, J. W. et al. Biotechnological potential of Korean marine microalgal strains and its future prospectives. *Ocean Polar Res.* **41**, 289–309 (2019).
31. Deethae, A., Peerapornpisal, Y., Pekkoh, J., Sangthong, P. & Tragoolpua, Y. Inhibitory effect of *Spirogyra* spp. algal extracts against herpes simplex virus type 1 and 2 infection. *J. Appl. Microbiol.* **124**, 1441–1453 (2018).
32. Dubois, M., Gilles, K. A., Hamilton, J. K., Rebers, P. A. & Smith, F. A colorimetric method for the determination of sugars. *Nature* **168**, 167 (1951).
33. Bradford, M. M. A rapid and sensitive method for the quantitation of microgram quantities of protein utilizing the principle of protein-dye binding. *Anal. Biochem.* **72**, 248–254 (1976).
34. Bennett, A. & Bogorad, L. Complementary chromatic adaptation in a filamentous blue-green alga. *J. Cell Biol.* **58**, 419–435 (1973).
35. Stunda-Zujeva, A., Berele, M., Lece, A. & Šķesters, A. Comparison of antioxidant activity in various spirulina containing products and factors affecting it. *Sci Rep.* **13**, 4529 (2023).
36. Rahman, I., Kode, A. & Biswas, S. K. Assay for quantitative determination of glutathione and glutathione disulfide levels using enzymatic recycling method. *Nat. Protoc.* **1**, 3159–3165 (2006).
37. Zhong, B. et al. 2020 LC-ESI-QTOF-MS/MS characterization of seaweed phenolics and their antioxidant potential. *Mar. Drugs* **18**, 331 (2020).
38. Ngu, E. L. et al. *Spirulina platensis* suppressed iNOS and proinflammatory cytokines in lipopolysaccharide-induced BV2 microglia. *Metabolites* **12**, 1147 (2022).
39. Srisai, P., Suriyaprom, S., Panya, A., Pekkoh, J. & Tragoolpua, Y. Inhibitory effects of algal polysaccharide extract from *Cladophora* spp. against herpes simplex virus infection. *Sci. Rep.* **14**, 11914 (2024).
40. Connelly, A. N. et al. Optimization of methods for the accurate characterization of whole blood neutrophils. *Sci Rep.* **12**, 3667 (2022).
41. Suriyaprom, S. et al. Antioxidant and anti-inflammatory activity on LPS-stimulated RAW264.7 macrophage cells of white mulberry (*Morus alba* L.) leaf extracts. *Molecules* **28**, 4395 (2023).
42. Joo, T. et al. Inhibition of nitric oxide production in LPS-stimulated RAW2647 cells by stem bark of *Ulmus pumila* L.. *Saudi J. Biol. Sci.* **21**, 427–435 (2014).
43. Han, S. et al. Procyanidin A1 alleviates inflammatory response induced by LPS through NF-κB, MAPK, and Nrf2/HO-1 pathways in RAW264.7 cells. *Sci. Rep.* **9**, 15087 (2019).
44. Baek, S. H., Park, T., Kang, M. G. & Park, D. Anti-inflammatory activity and ROS regulation effect of sinapaldehyde in LPS-stimulated RAW264.7 macrophages. *Molecules* **25**, 4089 (2020).
45. De Leon, J. A. D. & Borges, C. R. Evaluation of oxidative stress in biological samples using the thiobarbituric acid reactive substances assay. *J. Vis. Exp.* **159**, 10–3791. https://doi.org/10.3791/61122 (2020).
46. Butzer, U. et al. Increased oxidative stress in the RAW 264.7 macrophage cell line is partially mediated via the S-nitrosothiol-induced inhibition of glutathione reductase. *FEBS Lett.* **445**, 274–278 (1999).
47. Piao, S., Cha, Y. N. & Kim, C. Taurine chloramine protects RAW 264.7 macrophages against hydrogen peroxide-induced apoptosis by increasing antioxidants. *J. Clin. Biochem. Nutr.* **49**, 50–56 (2011).
48. Jaeschke, D. P., Teixeira, I. R., Marczak, L. D. F. & Mercali, G. D. Phycocyanin from Spirulina: A review of extraction methods and stability. *Food Res Int.* **143**, 110314 (2021).
49. Rahim, A. et al. Chemical characterization and nutritional value of *Spirulina platensis* cultivated in natural conditions of Chichaoua region (Morocco). *S. Afr. J. Bot.* **141**, 235–242 (2021).
50. Prete, V. et al. Beneficial effects of Spirulina supplementation in the management of cardiovascular diseases. *Nutrients* **16**, 642 (2024).
51. Andriopoulos, V. et al. Total phenolic content, biomass composition, and antioxidant activity of selected marine microalgal species with potential as aquaculture feed. *Antioxidants.* **11**, 1320 (2022).
52. Di Giacomo, C., Malfa, G. A., Tomasello, B., Bianchi, S. & Acquaviva, R. Natural compounds and glutathione: Beyond mere antioxidants. *Antioxidants.* **12**, 1445 (2023).
53. Pini, E., Rossi, E., Cornaglia Ferraris, P. & Stradi, R. Synthesis of purine derivatives of potential immunomodulatory activity. *Boll Chim. Farm.* **139**, 107–113 (2000).
54. Geitgey, D. K., Melendez, A. J., Caldeira-Botelho, R., Kemp, M. L. & Henry, C. J. Purinergic signaling and purine base metabolism at the crossroads between immunity, metabolism, and cancer: A review. *ImmunoMedicine.* **3**, e1044 (2023).
55. Deyab, M. A., El-Sheekh, M. M., Hasan, R. S., Elsadany, A. Y. & Abu Ahmed, S. E. S. Phytochemical components of two cyanobacterial local strains. *Sci. J. Damietta Fac. Sci.* **11**, 67–75 (2021).
56. Macário, I. P. E. et al. Metabolic composition of the cyanobacterium *Nostoc muscorum* as a function of culture time: A 1H NMR metabolomics study. *Algal Res.* **66**, 102792 (2022).
57. Lomakool, S. et al. Biological activities and phytochemicals profiling of different cyanobacterial and microalgal biomass. *Biomass Conv. Bioref.* **13**, 4195–4211 (2023).
58. Ai, X. et al. Polysaccharides from *Spirulina platensis*: extraction methods, structural features and bioactivities diversity. *Int. J. Biol. Macromol.* **231**, 123211 (2023).
59. Wang, B. et al. Extraction of polysaccharide from *Spirulina* and evaluation of its activities. *J. Evid. Based Complementary Altern Med.* **2018**, 3425615 (2018).
60. Jönsson, M., Allahgholi, L., Sardari, R. R. R., Hreggviðsson, G. O. & Nordberg Karlsson, E. Extraction and modification of macroalgal polysaccharides for current and next-generation applications. *Molecules* **25**, 930 (2022).
61. Chen, Y. et al. Extraction optimization of polysaccharides from wet red microalga *Porphyridium purpureum* using response surface methodology. *Mar. Drugs.* **22**, 498 (2024).
62. Wu, X. et al. Immunostimulatory effects of polysaccharides from Spirulina platensis in vivo and vitro and their activation mechanism on RAW246.7 macrophages. *Mar. Drugs* **18**, 538 (2020).
63. Han, B. et al. Protective effects of polysaccharides from *Spirulina platensis* against ultraviolet light-induced skin photoaging in KM mice and damage to mouse dermal fibroblasts. *J. Funct. Foods.* **129**, 106909 (2025).
64. Rechter, S. et al. Antiviral activity of *Arthrospira*-derived spirulan-like substances. *Antiviral Res.* **72**, 197–206 (2006).
65. Mader, J. et al. Calcium spirulan derived from *Spirulina platensis* inhibits herpes simplex virus 1 attachment to human keratinocytes and protects against herpes labialis. *J. Allergy Clin. Immunol.* **137**, 197-203.e3 (2016).

66. Adjali, A., Clarot, I., Chen, Z., Marchioni, E. & Boudier, A. Physicochemical degradation of phycocyanin and means to improve its stability: a short review. *J. Pharm. Anal.* **12**, 406–414 (2022).
67. Raichani, N. E., Guiraut, C., Morin, G., Mohamed, I. & Lavoie, J. C. Stability of glutathione added as a supplement to parenteral nutrition. *JPEN J. Parenter. Enteral. Nutr.* **46**, 1080–1087 (2022).
68. Bittner, M., Štern, A., Smutná, M., Hilscherová, K. & Žegura, B. Cytotoxic and genotoxic effects of cyanobacterial and algal extracts-microcystin and retinoic acid content. *Toxins.* **13**, 107 (2021).
69. Liu, P., Lee, M. K., Choi, J. W., Choi, Y. H. & Nam, T. J. Crude protein from spirulina increases the viability of CCD-986sk cells via the EGFR/MAPK signaling pathway. *Int. J. Mol. Med.* **43**, 771–778 (2019).
70. Jeong, Y. et al. Marine cyanobacterium *Spirulina maxima* as an alternate to the animal cell culture medium supplement. *Sci. Rep.* **11**, 4906 (2021).
71. Martínez-Ruiz, M. et al. Microalgae bioactive compounds to topical applications products-a review. *Molecules* **27**, 3512 (2022).
72. Bouyahya, A. et al. Bioactive substances of cyanobacteria and microalgae: sources, metabolism, and anticancer mechanism insights. *Biomed. Pharmacother.* **170**, 115989 (2024).
73. Serreli, G. & Deiana, M. Role of dietary polyphenols in the activity and expression of nitric oxide synthases: a review. *Antioxidants.* **12**, 147 (2023).
74. Intharuksa, A., Kuljarusnont, S., Sasaki, Y. & Tungmunnithum, D. Flavonoids and other polyphenols: bioactive molecules from traditional medicine recipes/medicinal plants and their potential for phytopharmaceutical and medical application. *Molecules* **29**, 5760 (2024).
75. Chei, S. et al. *Spirulina maxima* extract prevents activation of the NLRP3 inflammasome by inhibiting ERK signaling. *Sci. Rep.* **10**, 2075 (2020).
76. Kang, M. S., Moon, J. H., Park, S. C., Jang, Y. P. & Choung, S. Y. *Spirulina maxima* reduces inflammation and alveolar bone loss in *Porphyromonas gingivalis*-induced periodontitis. *Phytomedicine* **81**, 153420 (2021).
77. Behairy, A. et al. Antioxidant and anti-inflammatory potential of spirulina and thymoquinone mitigate the methotrexate-induced neurotoxicity. *Naunyn. Schmiedebergs Arch. Pharmacol.* **397**, 1875–1888 (2024).
78. Matsui, M. S., Muizzuddin, N., Arad, S. & Marenus, K. Sulfated polysaccharides from red microalgae have antiinflammatory properties in vitro and in vivo. *Appl. Biochem. Biotechnol.* **104**, 13–22 (2003).
79. Laroche, C. Exopolysaccharides from microalgae and cyanobacteria: diversity of strains, production strategies, and applications. *Mar. Drugs.* **20**, 336 (2022).
80. Viola, A., Munari, F., Sánchez-Rodríguez, R., Scolaro, T. & Castegna, A. The metabolic signature of macrophage responses. *Front. immunol.* **10**, 1462 (2019).
81. Lee, C. H. & Choi, E. Y. Macrophages and inflammation. *J Rheum. Dis.* **25**, 11–18 (2018).
82. Uhliariková, I. et al. Structural characteristics and biological effects of exopolysaccharide produced by cyanobacterium *Nostoc* sp. *Int. J. Biol. Macromol.* **160**, 364–371 (2020).
83. Vital, A. L. et al. Dexamethasone prevents granulocyte-macrophage colony-stimulating factor-induced nuclear factor-kappaB activation, inducible nitric oxide synthase expression and nitric oxide production in a skin dendritic cell line. *Mediators Inflamm.* **12**, 71–78 (2003).
84. Jeon, Y. J. et al. Dexamethasone inhibits IL-1 beta gene expression in LPS-stimulated RAW 264.7 cells by blocking NF-kappa B/Rel and AP-1 activation. *Immunopharmacology* **48**, 173–183 (2000).
85. Kumar, A. et al. Antioxidant and phytonutrient activities of *Spirulina platensis*. *Energy Nexus.* **6**, 1–9 (2022).
86. Yang, X. et al. The heart as a target for deltamethrin toxicity: inhibition of Nrf2/HO-1 pathway induces oxidative stress and results in inflammation and apoptosis. *Chemosphere* **300**, 134479 (2022).
87. Althobaiti, F. et al. Exploring the NRF2/HO-1 and NF-κB pathways: *Spirulina* nanoparticles as a novel approach to combat diabetic nephropathy. *ACS Omega* **9**, 23949–23962 (2024).
88. Jerez-Martel, I. et al. Phenolic profile and antioxidant activity of crude extracts from microalgae and cyanobacteria strains. *J. Food Qual.* **2017**, 2924508 (2017).
89. Ismaiel, M. M. S., El-Ayouty, Y. M. & Piercey-Normore, M. D. Antioxidants characterization in selected cyanobacteria. *Ann. Microbiol.* **64**, 1223–1230 (2014).
90. Cameron, J. C. & Pakrasi, H. B. Essential role of glutathione in acclimation to environmental and redox perturbations in the cyanobacterium *Synechocystis* sp. PCC 6803. *Plant Physiol.* **154**, 1672–1685 (2010).
91. Boden, J. S., Konhauser, K. O., Robbins, L. J. & Sánchez-Baracaldo, P. Timing the evolution of antioxidant enzymes in cyanobacteria. *Nat. Commun.* **12**, 4742 (2021).
92. Vignaud, J. et al. Microalgae produce antioxidant molecules with potential preventive effects on mitochondrial functions and skeletal muscular oxidative stress. *Antioxidants*. **12**, 1050 (2023).
93. Hsieh, I. T. et al. Enhanced stability, antioxidant capacity and in vivo anti-inflammatory efficacy of glutathione and quercetin via nanoemulsion formulation. *J. Taiwan Inst. Chem. Eng.* **168**, 105943 (2025).
94. Yang, K. C., Wu, C. C., Chen, W. Y., Sumi, S. & Huang, T. L. L-Glutathione enhances antioxidant capacity of hyaluronic acid and modulates expression of pro-inflammatory cytokines in human fibroblast-like synoviocytes. *J. Biomed. Mater. Res. A.* **104**, 2071–2079 (2016).
95. Silvagno, F., Vernone, A. & Pescarmona, G. P. The role of glutathione in protecting against the severe inflammatory response triggered by COVID-19. *Antioxidants.* **9**, 624 (2020).
96. Dawi, J. et al. Oxidative stress, glutathione insufficiency, and inflammatory pathways in type 2 diabetes mellitus: Implications for therapeutic interventions. *Biomedicines.* **13**, 18 (2025).
97. Tajvidi, E. et al. Study the antioxidant effects of blue-green algae Spirulina extract on ROS and MDA production in human lung cancer cells. *Biochem. Biophys. Rep.* **28**, 101139 (2021).
98. Lee, H. Y. et al. Protective effect of water extracted *Spirulina maxima* on glutamate-induced neuronal cell death in mouse hippocampal HT22 cell. *Pharmacogn. Mag.* **14**, 242–247 (2018).
99. Khan, M. et al. Spirulina attenuates cyclosporine-induced nephrotoxicity in rats. *J. Appl. Toxicol.* **26**, 444–451 (2006).
100. Park, J. H., Lee, S. I. & Kim, I. H. Effect of dietary *Spirulina* (*Arthrospira*) *platensis* on the growth performance, antioxidant enzyme activity, nutrient digestibility, cecal microflora, excreta noxious gas emission, and breast meat quality of broiler chickens. *Poult. Sci.* **97**, 2451–2459 (2018).
101. Zhang, L., Virgous, C. & Si, H. Synergistic anti-inflammatory effects and mechanisms of combined phytochemicals. *J. Nutr. Biochem.* **69**, 19–30 (2019).
102. Rajčević, N., Bukvički, D., Dodoš, T. & Marin, P. D. Interactions between natural products–A review. *Metabolites* **12**, 1256 (2022).
103. Begum, N. et al. Nutritional composition and functional properties of *A. platensis*-derived peptides: a green and sustainable protein-rich supplement. *Processes.* **12**, 2608 (2024).

Acknowledgements

This research was partially supported by Chiang Mai University, Targeted Research (TGCMU2566P017/2566) and Green Diamond Co., Ltd. are also acknowledged for their financial support. We would like to thank the Teaching Assistant and Research Assistant (TA/RA) Scholarship, the Graduate School Chiang Mai University, Chiang Mai, Thailand and Multidisciplinary and Interdisciplinary School, Chiang Mai University, Chiang Mai,

Thailand. Moreover, Natural Extracts and Innovative Products for Alternative Healthcare, and Cell Engineering for Cancer Therapy Research Groups, Chiang Mai University, Chiang Mai, Thailand were also grateful acknowledged. We would like to thank Sitthisak Intarasit and Waranut Buncharoen for providing the chemicals used in the antioxidative stress experiment.

Author contributions

P.S. contributed to the conceptualization, methodology, formal analysis and investigation, collection of resources, wrote the original draft, and edited the manuscript. S.S. performed formal analysis, investigation, and reviewed and edited the manuscript. S.K., A.P. and H.B. supervised the project. Y.T. was responsible for the conceptualization, methodology, formal analysis and investigation, reviewed and edited the manuscript, funding acquisition, and supervision. All authors read and approved the manuscript for submission.

Funding

Targeted Research, Chiang Mai University, TGCMU2566P017/ 2566, TGCMU2566P017/2566.

Declarations

Competing Interests

The authors declare no competing interests.

Additional information

Supplementary Information The online version contains supplementary material available at https://doi.org/10.1038/s41598-025-27372-4.

Correspondence and requests for materials should be addressed to Y.T.

Reprints and permissions information is available at www.nature.com/reprints.

Publisher's note Springer Nature remains neutral with regard to jurisdictional claims in published maps and institutional affiliations.